Chapter 10
Spectroscopy

Abstract Spectroscopy is an important experimental technique for determining properties of atoms and molecules, predominantly by means of their interaction with electromagnetic waves. The foundations of spectroscopy are closely related to the quantum states of matter; thus, the basic concepts in part recapitulate the contents of quantum mechanics (Chap. 9). The presented set of problems deals with different kinds of spectroscopy in the various regions of the electromagnetic spectrum. One focus is on problems that demonstrate how quantitative analysis of spectra provides detailed information on molecular structure and bonding. Other problems deal with the principle and dynamics of the laser, which is the most important laboratory light source in contemporary spectroscopy.

10.1 Basic Concepts

10.1.1 Fundamental Interaction Process Between Light and Matter

There are three basic types of interaction between an electromagnetic wave (frequency ν, wave vector $\mathbf{k}$) or a photon (energy $E = h\nu$, momentum $\mathbf{p} = \hbar\mathbf{k}$) and matter, i.e., an atom or molecule. The latter are represented by a two-level system.[1] These three types are illustrated in Fig. 10.1.

Induced absorption of a photon causes an excitation of the atom or molecule from a state of lower energy to a state of higher energy. **Spontaneous emission**, in contrast, is the transition of the atom or molecule from a state of higher energy to a state of lower energy under emission of a photon. A third process, called **induced emission**, is the transition from an excited state to a state of lower energy induced by a photon under emission of a second photon. Conservation of energy and momentum are guaranteed by the basic rules of quantum mechanics.[2] A transition is possible if the appropriate **selection rules** are fulfilled. The photon frequency involved with the transition is then related to the difference in energy between the two states E_{final}

[1] We have dealt with a quantum mechanical description of a two-level system in Problem 9.11.

[2] Energy conservation in absorption and emission processes is guaranteed in the limit $t \to \infty$.

J. Vogt, *Exam Survival Guide: Physical Chemistry*,
DOI 10.1007/978-3-319-49810-2_10

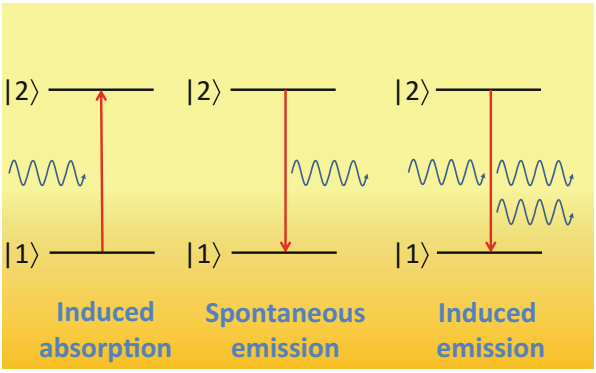

Fig. 10.1 The fundamental processes of interaction of matter with light. Matter is represented by an atomic or molecular two-level system that absorbs or emits photons

and E_{initial} of the atom or molecule. For the absorption, the photon frequency is:

$$h\nu = E_{\text{final}} - E_{\text{initial}}; \qquad E_{\text{final}} > E_{\text{initial}}. \tag{10.1}$$

For emission processes,

$$h\nu = E_{\text{initial}} - E_{\text{final}}; \qquad E_{\text{initial}} > E_{\text{final}}. \tag{10.2}$$

Experimentally, the absorption of light is measured by the attenuated spectral intensity $I(\nu)$ of an electromagnetic wave traveling through a medium of **optical depth** τ:

$$I(\nu) = I_0(\nu) \exp(-\tau) \tag{10.3}$$

$I_0(\nu)$ is the spectral intensity of the light source measured without an absorbing medium. Ideally, the optical depth τ depends on the length of the optical path L, the number density $\mathcal{N}$ of the absorbing species, and its **attenuation cross section** $\sigma(\nu)$:

$$\tau(\nu) = \mathcal{N}\, \sigma(\nu)\, L. \tag{10.4}$$

Equation (10.3) is called **Lambert Beer law**. Other related quantities common in absorption spectroscopy are the **transmittance**

$$T(\nu) = \frac{I(\nu)}{I_0(\nu)} \tag{10.5}$$

and the spectral **absorbance**

$$A_{10}(\nu) = -\log_{10} T(\nu). \tag{10.6}$$

Note that in the literature the absorbance is sometimes based on the natural logarithm, $A_e(\nu) = -\ln T(\nu)$. Moreover, in the presence of light beam attenuation due to scattering losses, the terminus **extinction** or **attenuance** is used instead of the absorbance.

Moreover, a quantitative description of absorption and emission processes sketched in Fig. 10.1 can be based on rate equations involving the spectral energy density of the electromagnetic field, $u(\nu)$, and the Einstein coefficients. The probability per second that an atom or molecule absorbs a photon of frequency ν is given by:

$$\frac{dP_{12}}{dt} = B_{12}u(\nu) \tag{10.7}$$

where B_{12} is the Einstein coefficient for induced absorption. Accordingly, the probability per second for induced emission of an excited atom or molecule is:

$$\frac{dP_{21}}{dt} = B_{21}u(\nu) \tag{10.8}$$

where B_{21} is the Einstein coefficient for induced emission. The probability per second of spontaneous emission does not depend on the energy density of the electromagnetic field:

$$\frac{dP_{21}}{dt} = A_{21} \tag{10.9}$$

A_{21} is the respective Einstein coefficient for spontaneous emission. The **lifetime** τ of the excited state with regard to spontaneous emission is:

$$\tau = \frac{1}{A_{21}}. \tag{10.10}$$

Higher order processes involve the absorption and emission of more than one photon. Light scattering processes, for example, are based on the absorption of a photon under excitation of the scattering atom or molecule on a **virtual intermediate state**, followed by the emission of a second photon and the subsequent transition back to the initial state (Rayleigh scattering), or to another final state (Raman scattering). Raman scattering is illustrated in Fig. 10.2 for the case of Stokes scattering and anti-Stokes scattering.

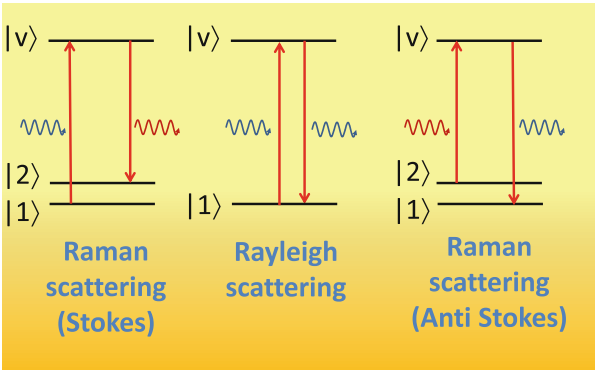

Fig. 10.2 Light scattering processes. Stokes scattering (*left*) starts from a low-lying initial state, and the emitted photon has a lower frequency than the absorbed one (red shift). Rayleigh scattering (*middle*) involves the same level as the final and initial state. Anti-Stokes scattering (*right*) starting from a state of higher energy results in a blue shift of the emitted photon

10.1.2 Rotational Spectroscopy: The Rigid Rotator

The simplest quantum mechanical model associated with molecular rotation is the diatomic rigid rotator outlined in Fig. 10.3. Its energy levels are given by:

$$E_J = hBJ(J+1) \qquad J = 0, 1, 2, \ldots \tag{10.11}$$

where J is the rotational quantum number, and B is the rotational constant in frequency units:

$$B = \frac{h}{8\pi^2 I} \tag{10.12}$$

B is related to the rotator's moment of inertia

$$I = \mu r^2 \tag{10.13}$$

with the effective mass μ depending on the masses of the two centers:

$$\mu = \frac{m_1 m_2}{m_1 + m_2} \tag{10.14}$$

As textbooks show, the solutions of the Schrödinger equation for the dumbbell-shaped rigid rotator are the spherical harmonics $Y_{JM}(\theta, \phi)$ (see Sect. A.3.14 in

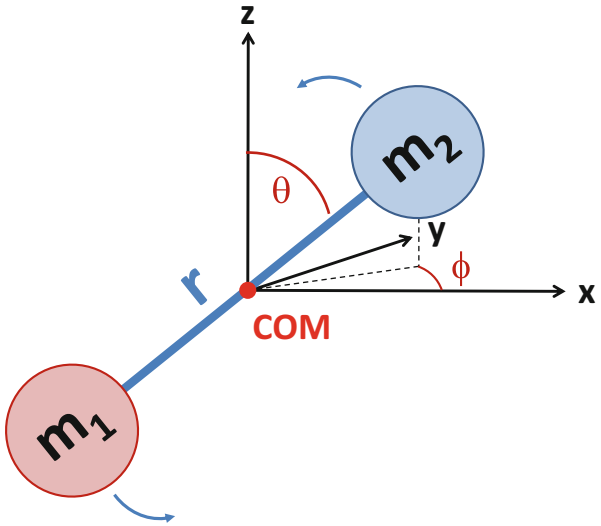

Fig. 10.3 The diatomic dumbbell-shaped rotator. The center of mass (COM) is the origin of the molecule-fixed coordinate system. The orientation of the molecule is fully described by the tilt angle θ and the azimuthal angle ϕ

the appendix). The two angles θ and ϕ completely define the orientation of the molecule. Because the energy levels Eq. (10.11) do not depend on the orientational quantum number M, they are degenerated. The degeneracy corresponds to the number $(2J + 1)$ of possible M values for a given J. Rotational transitions mediated by the absorption or emission of light are bound to selection rules. Pure rotational transitions require a permanent electric dipole moment and, moreover

$$\Delta J = \pm 1; \qquad \Delta M = 0, \pm 1. \tag{10.15}$$

As a consequence of the energy levels Eq. (10.11) and these selection rules, the pure rotation spectrum exhibits equidistant transitions, as shown in Fig. 10.4.

10.1.3 Vibrational Spectroscopy of Molecules

Key to the description of the vibrational spectroscopy of molecules is the model of the **harmonic oscillator** (see Sect. 9.1.2.3). Given a force constant k and an effective

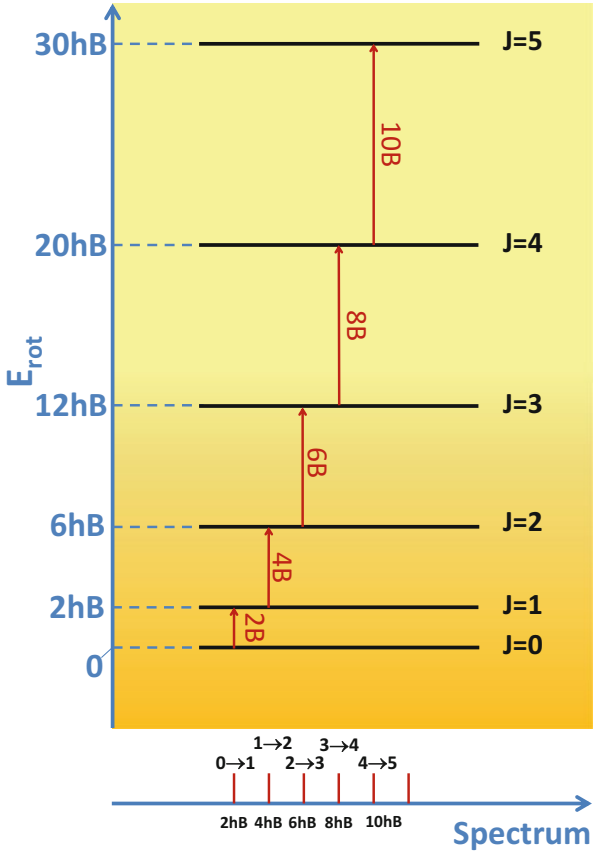

Fig. 10.4 The energy levels of the rigid diatomic rotator and the resulting spectrum of equidistant lines

mass μ, the harmonic oscillation frequency is

$$\nu_e = \frac{1}{2\pi}\sqrt{\frac{k}{\mu}}. \tag{10.16}$$

The quantum energy of the oscillator is $h\nu_e$ and the energy levels are

$$E_n = h\nu_e\left(n + \frac{1}{2}\right) \qquad n = 0, 1, 2, \ldots \tag{10.17}$$

where n is the vibrational quantum number. The selection rules for transitions of an harmonic oscillator between two states n and n' are:

$$\Delta n = n - n' = \pm 1. \tag{10.18}$$

Moreover, an *induced* electric dipole moment must be involved with the vibrational transition. **Anharmonicity** of the potentials between atomic cores lowers the energy of a vibrational transition. The generally observed relation (see Problem 10.6) is

$$E_n = h\nu_e \left(n + \frac{1}{2}\right) - x_e h\nu_e \left(n + \frac{1}{2}\right)^2 \tag{10.19}$$

where x_e is an anharmonicity constant.

10.2 Problems

Additional problems related to spectroscopy can be found in Chap. 9.

Problem 10.1 (Units of Measurement in Spectroscopy)
Different units of measurement are used in spectroscopy.

a. Clarify the relationship between energy (E), frequency (ν), wavelength (λ), and wave number ($\tilde{\nu}$).
b. For the following data, provide the missing values of E, ν, λ, and $\tilde{\nu}$. Assign the data to the respective range within the electromagnetic spectrum.

- $E = 1\,\text{eV}$.
- $\lambda = 21\,\text{cm}$ (hyperfine splitting of hydrogen)
- Room temperature thermal energy ($k_B T$, $T = 298.15\,\text{K}$).
- $\tilde{\nu} = 2170\,\text{cm}^{-1}$ (CO stretch vibration).
- $E = 13.6\,\text{eV}$ (ionization energy of the hydrogen atom).
- $E = 511\,\text{keV}$ (positron annihilation radiation).

Solution 10.1 In this exercise, we familiarize ourselves with the basic units used in spectroscopy. The use of different units in the various spectroscopic disciplines may seem confusing at first sight. However, depending on the range of the electromagnetic spectrum (Table 10.1), where transitions of atoms and molecules occur, some units are indeed more appropriate than others. In **subproblem (a)**, we give the relationships among energy, frequency, wavelength, and wave number. The

Table 10.1 The ranges of the electromagnetic spectrum

Range	Wavelength	Energy
Gamma rays	0–0.01 nm	124 keV–∞
X-rays	0.01–10 nm	124 eV–124 keV
Ultraviolet (UV)	10–380 nm	3.26–124 eV
Visible (Vis)	380–780 nm	1.59–3.26 eV
Infrared (IR)	780 nm–1 mm	1.24 meV–1.59 eV
Microwaves	1 mm–100 cm	1.24 μeV–1.24 meV
Radiowaves	100 cm–∞	0–1.24 μeV

relation between energy and frequency is established by:

$$E = h\nu \tag{10.20}$$

where $h = 6.62606957(29) \times 10^{-34}\,\mathrm{J\,s}$ is the Planck constant (see Sect. A.1 in the appendix). The relation between frequency and wavelength is:

$$\lambda\nu = c \tag{10.21}$$

where $c = 299{,}792{,}458\,\mathrm{m\,s^{-1}}$ is the vacuum speed of light.[3] Finally, the wave number is the reciprocal wavelength:

$$\tilde{\nu} = \frac{1}{\lambda}. \tag{10.22}$$

In **subproblem (b)**, we look at some instructive examples. The first example is the energy $E = 1\,\mathrm{eV}$, i.e., the kinetic energy, that a particle with charge e gains if it passes a potential difference of 1 V. This is the unit electron volt that is common in many spectroscopic disciplines. In SI units, this energy is $E = 1.60218 \times 10^{-19}\,\mathrm{J}$, and the frequency is:

$$\nu = \frac{E}{h} = 2.41799 \times 10^{14}\,\mathrm{Hz} \approx 242\,\mathrm{THz}.$$

The wavelength is:

$$\lambda = \frac{c}{\nu} = 1.23984 \times 10^{-6}\,\mathrm{m} \approx 1.24\,\mu\mathrm{m} = 1240\,\mathrm{nm}.$$

[3] In a dielectric medium with dielectric constant ϵ and permeability μ the speed of light is $\frac{c}{\sqrt{\epsilon\mu}}$.

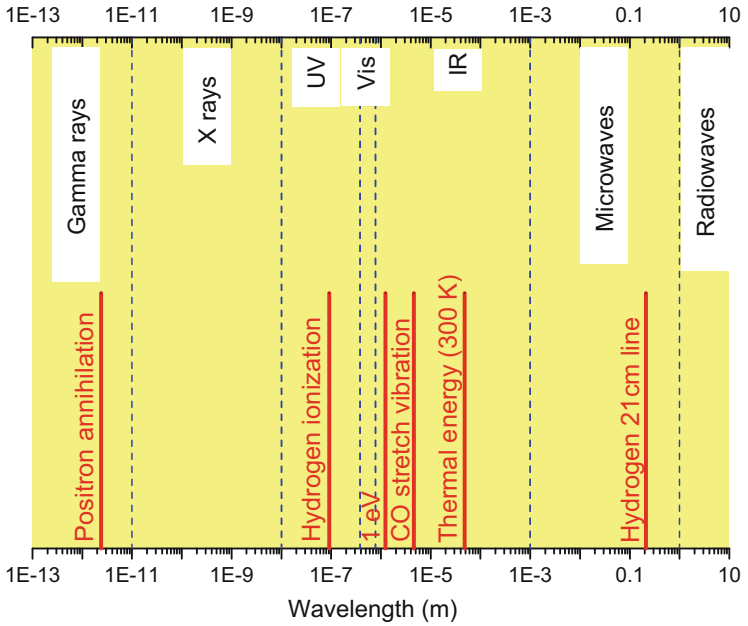

Fig. 10.5 Survey over the electromagnetic spectrum, classified according to the spectral ranges given in Table 10.1. Also indicated are the positions of characteristic spectroscopic transitions of Problem 10.1b

and the wave number is:

$$\tilde{\nu} = \frac{1}{\lambda} = 806{,}556\,\mathrm{m}^{-1} = 8065.56\,\mathrm{cm}^{-1}. \tag{10.23}$$

Note that it is more common to express the wave number in cm^{-1} than in m^{-1}.

We assign these values to the infrared range (IR); more precisely, the near infrared (NIR) range, as also indicated in Fig. 10.5 along with the other examples of this subproblem. The second example is the hyperfine splitting of hydrogen with its characteristic transition at $\lambda = 21\,\mathrm{cm}$, resulting from the *flipping* of the electron spin relative to the orientation of the nuclear spin. It is within the microwave spectral range of the electromagnetic spectrum. In radio astronomy the 21 cm line is key for the measurement of hydrogen in space. Conversion to wave number yields $\tilde{\nu} = 0.0476\,\mathrm{cm}^{-1}$, an energy of $E = 5.9\,\mu\mathrm{eV}$, and a frequency of $\nu = 1.4\,\mathrm{GHz}$. The third example is not related to a special transition, it is the thermal energy at room temperature,

$$E = k_B T = 1.38065 \times 10^{-23}\,\mathrm{J\,K}^{-1} \times 298.15\,\mathrm{K} = 4.11641 \times 10^{-21}\,\mathrm{J} = 25.69\,\mathrm{meV}.$$

To estimate if energy levels of atoms, molecules, or solids are populated at room temperature, comparison with this energy value is crucial (see Problem 9.15 at page 260). Room temperature thermal energy corresponds to a frequency of $\nu = 6.2 \times 10^{12}\,\mathrm{Hz}$, $\lambda = 48\,\mu\mathrm{m}$, and $\tilde{\nu} = 207\,\mathrm{cm}^{-1}$. It is thus located in the IR spectral range, more precisely, the mid infrared (MIR). The fourth example is related to the excitation of the stretch vibration of the carbon monoxide molecule at $\tilde{\nu} = 2170\,\mathrm{cm}^{-1}$. It is related to a wavelength $\lambda = 4.61\,\mu\mathrm{m}$, frequency $\nu = 6.51 \times 10^{13}\,\mathrm{Hz}$, and energy $E = 0.269\,\mathrm{eV}$. This transition is thus also located in the mid infrared spectral range. In fact, IR spectroscopy is the key method for measuring vibrational transitions of molecules. The fifth example is the well-known ionization energy of atomic hydrogen, $E = 13.6\,\mathrm{eV}$. Also known as Rydberg energy (see Eq. (9.22)), this energy is important in quantum chemistry. The corresponding frequency is $\nu = 3.29 \times 10^{15}\,\mathrm{Hz}$, the wavelength is $\lambda = 91.2\,\mathrm{nm}$, and the wave number is[4] $\tilde{\nu} = 109{,}691\,\mathrm{cm}^{-1}$. The ionization energy of hydrogen is thus assigned to the ultraviolet spectral range. The last example is positron annihilation radiation, corresponding to the characteristic energy $E = 511\,\mathrm{keV}$ in the gamma ray spectral range. The radiation is the result of the reaction:

$$\mathrm{e}^+ + \mathrm{e}^- \longrightarrow 2\gamma$$

producing two γ photons.[5] The frequency of the photons is $\nu = 1.2 \times 10^{20}\,\mathrm{Hz}$, the wavelength is $\lambda = 0.0024\,\mathrm{nm}$, and the wave number is $\tilde{\nu} = 4.12 \times 10^{9}\,\mathrm{cm}^{-1}$. These are quite extreme values. Nevertheless, gamma spectroscopy has important applications: in medicine, positron emission tomography (PET) is used as an imaging technique for metabolic processes in the body. Mößbauer spectroscopy has important applications in geology and metrology.

Problem 10.2 (Doppler Broadening of Spectral Lines)
Apart from a natural line width, a significant source of the broadening of spectral lines of atoms and molecules in the gas phase is caused by the Doppler effect. Compared with the frequency ν_0 of an external electromagnetic wave seen by a molecule or atom at rest, the frequency changes to:

$$\nu = \nu_0 \left(1 + \frac{v_x}{c}\right) \tag{10.24}$$

where v_x is the velocity component of the atom or molecule in line with the wave field, and $v_x \ll c$ (see Fig. 10.6).

(continued)

[4] The exact result, determined using $E = 13.605693\,\mathrm{eV}$ would be $109{,}737\,\mathrm{cm}^{-1}$.

[5] Conservation of energy and momentum requires the generation of two photons. Each photon has the energy $E = m_e c^2 = 9.10938 \times 10^{-31}\,\mathrm{kg} \times (299{,}792{,}458\,\mathrm{m\,s}^{-1})^2 \approx 511\,\mathrm{keV}$.

Problem 10.2 (continued)

a. Assume a Maxwell-Boltzmann velocity distribution of the gas particles and show that the Doppler effect causes a Gaussian line profile with half width

$$\Delta\nu = \frac{\nu_0}{c}\sqrt{\frac{8k_BT\ln 2}{m}} \tag{10.25}$$

where T is the temperature, and m the mass of the gas particles.

b. Calculate the Doppler line width of the rovibrational transition ($J = 1, n = 0 \longrightarrow J = 0, n = 1$) of carbon monoxide $^{12}C^{16}O$ found at 2,139.427 cm^{-1} at a temperature of 300 K.

c. For a temperature of 300 and 430 K, calculate the Doppler line widths of the sodium D_1 and D_2 lines found at 508.332466 and 508.848717 THz respectively.

Solution 10.2 This problem deals with the broadening of spectral lines of gaseous particles. The problem is also related to the kinetic theory of gases in Chap. 7. Although every spectral line has a natural line width owing to the finite lifetime of an excited state (see Eq. (10.10)), there are other mechanisms that lead to a further broadening of a spectral line. Significant broadening may be caused by the Doppler effect due to the thermal movement of the gas particles.

In **subproblem (a)**, we investigate the effect on the line profile in detail and find a proof of Eq. (10.25). We consider the simplified arrangement shown in Fig. 10.6, which is typical for absorption spectroscopy of atoms or molecules in the gas phase. We assume a number density $\mathcal{N}_{\text{tot}}$ and a transition of the molecules at a frequency ν_0 of arbitrary sharpness with an absorption cross section σ_0. If we consider the fictive case in which all molecules in the gas cell were at rest, then, according to Eq. (10.4),

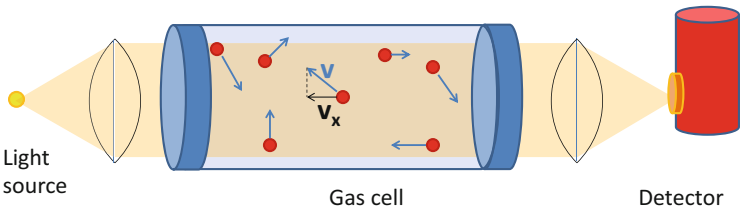

Fig. 10.6 Absorption spectroscopy probing atoms or molecules in a gas cell (schematic)

the optical depth would be a delta function centered around ν_0:

$$\tau(\nu - \nu_0) = \mathscr{N}_{\text{tot}} \delta(\nu - \nu_0) \sigma_0 L. \tag{10.26}$$

L is the length of the gas cell and $\delta(\nu - \nu_0)$ is Dirac's delta function centered at the frequency ν_0. The optical depth integrated over the whole frequency range, is:

$$\int_{-\infty}^{+\infty} \tau(\nu - \nu_0)\, d\nu = \mathscr{N}_{\text{tot}} \sigma_0 L \int_{-\infty}^{+\infty} \delta(\nu - \nu_0)\, d(\nu - \nu_0) \overset{\text{Eq. (A.52)}}{=} \mathscr{N}_{\text{tot}} \sigma_0 L. \tag{10.27}$$

Next, we take the motion of the molecules, which causes the Doppler effect, into account. If an emitter of a wave is in motion, the frequency of the wave is higher if the emitter moves toward the observer, and it is lower if the emitter goes in the opposite direction. Usually, textbooks show that this Doppler effect is a consequence of wave theory, but Eq. (10.24) can also be shown in a rigorous way in the photon picture of light, if we take into account the recoil of a photon emitting atom or molecule [1]. In absorption spectroscopy, however, the light source can be considered at rest, whereas the gas particle takes the role of the "observer" In this case, the same relation, Eq. (10.24) holds:

$$\nu = \nu_0 \left(1 + \frac{v_x}{c}\right) \tag{10.28}$$

Note that v_x is the velocity component of a certain molecule in line with the wave vector of the electromagnetic field. The fact that the field probes many molecules, each moving with a different velocity, is taken into account by assuming a Maxwell–Boltzmann distribution of the particle velocity. In Problem 7.1, we have seen that the velocity distribution for the velocity component in the x-direction is a normalized Gaussian distribution. Thus, the number density of particles with the velocity v_x is:

$$\mathscr{N}(v_x) = \mathscr{N}_{\text{tot}} \left(\frac{m}{2\pi k_B T}\right)^{\frac{1}{2}} \exp\left(-\frac{m}{2k_B T} v_x^2\right) dv_x = \frac{\mathscr{N}_{\text{tot}}}{\sqrt{\pi}\, v_m} \exp\left(-\frac{v_x^2}{v_m^2}\right) dv_x \tag{10.29}$$

Here, we have introduced the *most probable* velocity v_m derived in Eq. (7.19). We annotate that:

$$\int_{-\infty}^{+\infty} \mathscr{N}(v_x)\, dv_x = \frac{\mathscr{N}_{\text{tot}}}{v_m \sqrt{\pi}} \int_{-\infty}^{+\infty} \mathrm{e}^{-\frac{v_x^2}{v_m^2}}\, dv_x \overset{\text{Eq. (A.46)}}{=} \frac{\mathscr{N}_{\text{tot}}}{v_m \sqrt{\pi}} v_m \sqrt{\pi} = \mathscr{N}_{\text{tot}}. \tag{10.30}$$

The decisive step now is the transformation of this velocity distribution into a distribution of the number density as a function of resonance frequency. Dependent on v_x, the atom or molecule absorbs radiation at a slightly different frequency.

Solving Eq. (10.24) for v_x, we can make the following substitutions:

$$v_x = c\frac{\nu - \nu_0}{\nu_0} \tag{10.31}$$

and

$$dv_x = \frac{c}{\nu_0}\, d\,(\nu - \nu_0)\,. \tag{10.32}$$

Equation (10.30) may be written as:

$$\int_{-\infty}^{+\infty} \mathscr{N}(v_x)\, dv_x = \int_{-\infty}^{+\infty} \underbrace{\mathscr{N}_{\text{tot}} \frac{c}{\nu_0 v_m \sqrt{\pi}} \mathrm{e}^{-\left(\frac{c}{\nu_0 v_m}\right)^2 (\nu-\nu_0)^2}}_{\mathscr{N}(\nu-\nu_0)}\, d(\nu - \nu_0) \overset{\text{Eq. (A.46)}}{=} \mathscr{N}_{\text{tot}} \tag{10.33}$$

With the identified distribution function $\mathscr{N}(\nu - \nu_0)$ the optical depth analogous to Eq. (10.26) can be written:

$$\tau(\nu - \nu_0) = \mathscr{N}_{\text{tot}} \sigma_0 L \frac{c}{\nu_0 v_m \sqrt{\pi}} \mathrm{e}^{-\left(\frac{c}{\nu_0 v_m}\right)^2 (\nu-\nu_0)^2} \tag{10.34}$$

In comparison with the last equation with the *normal distribution* Eq. (A.64) found in the appendix, we can identify its *standard deviation*

$$\sigma = \frac{v_m}{\sqrt{2}} \frac{\nu_0}{c}. \tag{10.35}$$

The half-width of the Doppler-broadened spectral line is thus obtained using Eq. (A.65), which relates the half-width to the standard deviation:

$$\delta\nu = 2\sigma\sqrt{2\ln 2} = 2\frac{\nu_0}{c} v_m \sqrt{\ln 2} \tag{10.36}$$

If we replace v_m using Eq. (7.19), we finally obtain Eq. (10.25), which was shown.

In **subproblem (b)**, we calculate the expected Doppler width for a special rovibrational transition of the CO molecule at room temperature at $\tilde{\nu}_0 = 2139.427\,\text{cm}^{-1}$. Using the relation between wave number and frequency, $\tilde{\nu} = \frac{\nu}{c}$, we obtain the expression for the Doppler width in wave numbers, which is:

$$\Delta\tilde{\nu} = \frac{\tilde{\nu}_0}{c} \sqrt{\frac{8 k_B T \ln 2}{m}}. \tag{10.37}$$

Hence,

$$\sqrt{\frac{8k_BT\ln 2}{m}} = \sqrt{\frac{8 \times 1.38065 \times 10^{-23}\,\mathrm{J\,K^{-1}} \times 300\,\mathrm{K} \times 0.69315}{28 \times 1.66059 \times 10^{-27}\,\mathrm{kg}}} = 70{,}284\,\mathrm{cm\,s^{-1}}. \tag{10.38}$$

Therefore, the line width sought is:

$$\Delta\tilde{\nu} = \frac{2139.427\,\mathrm{cm^{-1}}}{29{,}979{,}245{,}800\,\mathrm{cm\,s^{-1}}} \times 70{,}284\,\mathrm{cm\,s^{-1}} = 0.005\,\mathrm{cm^{-1}}, \tag{10.39}$$

corresponding to $\Delta\nu = 48\,\mathrm{MHz}$. This result is in fact close to the observed line width at a low pressure in the gas cell. Note that in typical undergraduate spectroscopy laboratories the resolution is usually not sufficient to determine this line width. In these cases, the observed line width is mostly determined by the spectrometer itself.

In **subproblem (c)**, we deal with another example, the well-known sodium D-line doublet in the visible part of the electromagnetic spectrum. From the periodic table in the appendix, we take the atomic mass of sodium, 22.99 m_u. Thus,

$$\sqrt{\frac{8k_BT\ln 2}{m_{\mathrm{Na}}}} = \begin{cases} 775.6\,\mathrm{m\,s^{-1}};\ T = 300\,K \\ 928.6\,\mathrm{m\,s^{-1}};\ T = 430\,K \end{cases} \tag{10.40}$$

Using Eq. (10.25) and the given transition frequencies 508.332466 THz (D_1 line) and 598.848717 THz (D_2 line) respectively we obtain the values for the Doppler width shown in Table 10.2. The values are within the GHz range and are thus much smaller than for the splitting of this doublet. Experimentally, both line profiles would have a shoulder because the *hyperfine structure splitting* of the Na 3^2S ground state of 1.772 GHz is close to the experimental line width. The hyperfine structure of the excited state, in contrast, is usually not resolved with simple absorption spectroscopy. Measuring line widths has interesting technical applications: for example, the temperature dependence of the Doppler width (Eq. (10.25)) opens up the possibility of determining the temperature of flames from a spectroscopic measurement.

Table 10.2 Doppler line width of sodium D lines

	300 K	430 K
$\Delta\nu(D_1)$	1.315 GHz	1.575 GHz
$\Delta\nu(D_2)$	1.316 GHz	1.576 GHz

Problem 10.3 (UV Absorption of Proteins)
In biochemical analytics, the concentration of polypeptides can be determined by measuring their ultraviolet absorption at a wave length of 280 nm. At this wave length, the extinction coefficients of the amino acids tryptophan (Trp), tyrosine (Tyr), and cysteine (Cys) are: $\epsilon_{\text{Trp}} = 5690\,\text{M}^{-1}\,\text{cm}^{-1}$, $\epsilon_{\text{Tyr}} = 1280\,\text{M}^{-1}\,\text{cm}^{-1}$, $\epsilon_{\text{Cys}} = 120\,\text{M}^{-1}\,\text{cm}^{-1}$, respectively (S.C. Gill, P.H. von Hippel, Anal. Biochem. **182** (1989), 319; 1 M=z1 mol l^{-1}). According to the Lambert–Beer law, the absorbances A_i of these species are then given by:

$$A_i = \epsilon_i c_i L \tag{10.41}$$

where c_i is their concentration (unit: mol l^{-1}) and L the optical path length. Assume a path length of 1 cm.

a. A sample containing the enzyme glutamate dehydrogenase containing 4 units of Trp, 18 units of Tyr, and 6 units of Cys absorbs 30% of the incoming radiation. Calculate the concentration of the enzyme.
b. Oxytocin ($C_{43}H_{66}N_{12}O_{12}S_2$) contains 2 units of Cys and 1 unit of Tyr. What is the absorbance of a sample of 1 l solution containing 1 g oxytocin?

Solution 10.3 This exercise deals with a concrete application of optical absorption spectroscopy in chemical analytics. =In Problem 9.13, we have dealt with the UV absorption of benzene due to electronic excitation of its system of π electrons. Amino acids with rings such as Trp and Tyr (see Fig. 10.7) absorb light within the ultraviolet spectral range at a wave length of 280 nm. Cysteine also weakly absorbs light at this wave length. As these molecules are found in the amino acid sequences of larger protein structures, their UV absorption can be used for a quantitative analysis. In **subproblem (a)**, we determine the concentration of glutamate dehydrogenase in a sample that absorbs 30% of the incoming light at a wave length of 280 nm. According to Eqs. (10.5) and (10.6), the absorbance is:

$$A = -\log_{10}\frac{I}{I_0} = -\log_{10}\frac{1-0.3}{1} = 0.155 \tag{10.42}$$

At least at low concentrations[6], this total absorbance can be taken as the sum of the absorbances of the three active subunits Cys, Trp, and Tyr:

$$A = \sum_i A_i = L\sum_i \epsilon_i c_i \tag{10.43}$$

[6] At high concentrations the effects of scattering including multiple scattering events need to be taken into account.

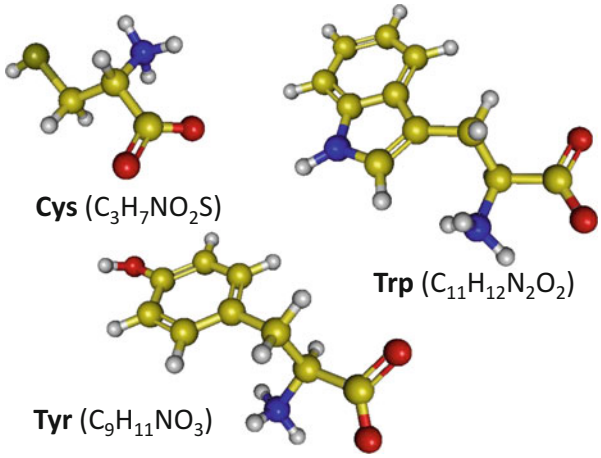

Fig. 10.7 Molecular structure of the three amino acids cysteine (Cys), tyrosine (Tyr), and tryptophan (Trp)

If $z_{\mathrm{Cys}} = 6$, $z_{\mathrm{Tyr}} = 18$, and $z_{\mathrm{Trp}} = 4$ are the numbers of Cys, Tyr, and Trp units in glutamate dehydrogenase and c is the sought concentration of this enzyme, we have

$$A = Lc \sum_i \epsilon_i z_i \tag{10.44}$$

and thus

$$\begin{aligned} c &= \frac{A}{L \sum_i \epsilon_i z_i} = \frac{0.155}{1\,\mathrm{cm}\,(4 \times 5690 + 18 \times 1280 + 6 \times 120)\ \mathrm{M}^{-1}\,\mathrm{cm}^{-1}} \\ &= 3.33 \times 10^{-6}\,\mathrm{M}. \end{aligned} \tag{10.45}$$

In **subproblem (b)**, the absorbance of a sample of 1 g oxytocin in 1 l solution is calculated. Thus, we must determine the molar mass of this molecule. From the formula $C_{43}H_{66}N_{12}O_{12}S_2$, we obtain the molar mass M=1007 g mol^{-1}. Thus, the concentration of the sample is $c = 9.9 \times 10^{-4}$ M. As the molecule contains 2 units of Cys and 1 unit of Tyr, the sought absorbance of a sample is:

$$\begin{aligned} A &= Lc\left(2\epsilon_{\mathrm{Cys}} + \epsilon_{\mathrm{Tyr}}\right) = 1\,\mathrm{cm} \times 9.9 \times 10^{-4}\,\mathrm{M}\,(2 \times 120 + 1280)\ \mathrm{M}^{-1}\,\mathrm{cm}^{-1} \\ &= 1.5, \end{aligned} \tag{10.46}$$

which is a large value. The transmitted intensity would be only $I = I_0\, 10^{-1.5} = 0.03\, I_0$.

Problem 10.4 (HCN Molecular Structure)
By means of microwave spectroscopy, the following rotational constants for various isotopomers of the linear HCN molecule were determined (E.F. Pearson et al., Z. Naturforsch. **31a** (1976), 1394): $H^{13}C^{14}N$: $B_0 = 43170.140\,\text{MHz}$; $H^{12}C^{14}N$: $B_0 = 44315.9757\,\text{MHz}$.

a. Find expressions for the positions of the atomic cores with regard to the molecule's center of mass.
b. Find an expression for the moment of inertia in the center of mass frame of reference that depends only on the nuclear masses and the bond length r_{CN} and r_{CH}.
c. Provided that the Born-Oppenheimer approximation is valid for the ground state of HCN, the bond lengths are not affected by different isotopic masses. Determine the bond lengths in the HCN ground state. *Hint: use an iterative procedure or mathematical software to solve the system of equations.*

Solution 10.4 In this problem, we deal with the structure determination of a linear triatomic molecule: HCN (Fig. 10.8). The goal is to determine the bond lengths of the C-H and the C-N bond by the measurement of the rotational constants from at least two different isotopomers. These have different nuclear masses, but it can be expected that the bond lengths, which are only determined by electronic structure,[7] are the same. This is a consequence of the Born-Oppenheimer approximation, according to which the total wave function of a molecule (electronic and nuclear degrees of freedom) can be separated into a nuclear part and an electronic part.

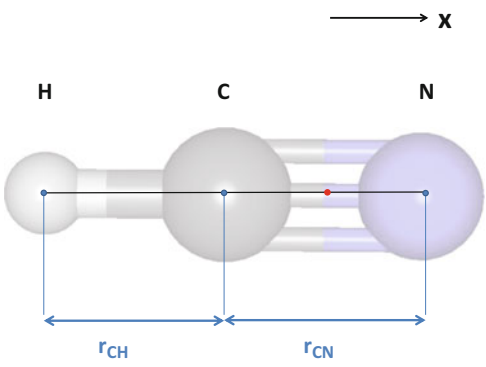

Fig. 10.8 The linear structure of the HCN molecule. The center of mass, indicated by the *red dot*, is along the C-N bond

[7] See Problem 9.18 dealing with chemical bonding in the simplest possible molecular system, the H_2^+ molecule ion.

In **subproblem (a)** we begin by searching expressions for the positions of the three nuclei in the center of mass frame of reference. Note that for different isotopomers the center of mass is at different positions on the molecular axis of symmetry. We need them to form the moments of inertia, which in turn are related to the rotational constants (see Eq. (10.12)). The center of mass, indicated as a dot in Fig. 10.8, lies between the heavier carbon and nitrogen cores. It is thus reasonable to tentatively set the origin at the carbon site. This choice sets $\tilde{x}_C = 0$, $\tilde{x_N} = r_{CN}$, $\tilde{x_H} = -r_{CH}$. The position of the center of mass in this system is:

$$\tilde{x}_{COM} = \frac{m_H \tilde{x}_H + m_C \tilde{x}_C + m_N \tilde{x}_N}{M} = \frac{m_N r_{CN} - m_H r_{CH}}{M}$$

where $M = m_H + m_C + m_N$ is the total mass of the molecule. In the new frame of reference centered at the molecular center of mass, the positions of the atoms are thus:

$$x_H = -\frac{m_N r_{CN} - m_H r_{CH}}{M} - r_{CH} = x_C - r_{CH} \tag{10.47}$$

$$x_C = -\frac{m_N r_{CN} - m_H r_{CH}}{M} \tag{10.48}$$

$$x_N = -\frac{m_N r_{CN} - m_H r_{CH}}{M} + r_{CN} = x_C + r_{CN} \tag{10.49}$$

In **subproblem (b)**, we write down the moment of inertia in the center of mass frame of reference. The moments of inertia of the molecule are $I_{xx} = 0, I_{yy} = I_{zz} = I$ where

$$I = m_N (r_{CN} + x_C)^2 + m_C x_C^2 + m_H (x_C - r_{CH})^2 \tag{10.50}$$

The goal is to write this as an expression that contains only the known masses of the nuclei and the bond lengths r_{CH} and r_{CN}. Using Eq. (10.48), we substitute the position of the carbon, x_C. After some algebra, we obtain:

$$I = \left(m_N - \frac{m_N^2}{M}\right) r_{CN}^2 + \left(m_H - \frac{m_H^2}{M}\right) r_{CH}^2 + \frac{2 m_N m_H}{M} r_{CN} r_{CH} \tag{10.51}$$

This equation gives the relation of the moment of inertia with the bond lengths and the masses. On the other hand, I is related to the rotational constant:

$$I = \frac{h}{8\pi^2 B_0} \tag{10.52}$$

With two different rotational constants for two different sets of nuclear masses, we have two equations for the two unknown bond lengths:

$$I_1 = A_1 r_{\mathrm{CN}}^2 + B_1 r_{\mathrm{CH}}^2 + C_1 r_{\mathrm{CN}} r_{\mathrm{CH}} \tag{10.53}$$

$$I_2 = A_2 r_{\mathrm{CN}}^2 + B_2 r_{\mathrm{CH}}^2 + C_2 r_{\mathrm{CN}} r_{\mathrm{CH}} \tag{10.54}$$

where $A_i = \left(m_{\mathrm{N},i} - \frac{m_{\mathrm{N},i}^2}{M_i} \right)$, $B_i = \left(m_{\mathrm{H},i} - \frac{m_{\mathrm{H},i}^2}{M_i} \right)$, and $C_i = \frac{2 m_{\mathrm{N},i} m_{\mathrm{H},i}}{M_i}$, $i = 1, 2$ are *effective masses*.

Unfortunately, these equations are not linear in the bond lengths. Thus, we have to seek the solutions numerically. This is tackled in **subproblem (c)**. In the appendix, Sect. A.3.19, Newton's method for the solution of a nonlinear system of equations is described. A computer code is easily set up that implements Newton's method for this problem. The output from such a computer code is shown below. Starting from a reasonable initial guess of the bond lengths of 1 Å for both bonds, Newton's method converges within about 10 iterations toward $r_{\mathrm{CN}} = 1.1569$ Å and $r_{\mathrm{CH}} = 1.0689$ Å. As can be seen in the output, the exchange of ^{12}C with ^{13}C changes the nuclei's positions relative to the center of mass by about 0.02 Å. The calculation is for a perfectly rigid rotator. Even in the vibrational ground state, however, a slight correction of the rotational constants originating from rotation vibration coupling is present. Such corrections are considered in Problem 10.7. As shown there, these corrections change the bond lengths obtained to the order of 10^{-3} Å.

Newton's iterative method output

```
HCN molecule bond length fit from rotational constants
------------------------------------------------------
Set 1 of parameters
Mass hydrogen (AMU)=           1
Mass carbon (AMU)  =          12
Mass nitrogen (AMU)=          14
Rotational constant CONSTANT (MHz):   44,315.975700000003
------------------------------------------------------
Set 2 OF parameters
Mass hydrogen (AMU)=           1
Mass carbon (AMU)  =          13
Mass nitrogen (AMU)=          14
Rotational constant (MHz):   43,170.139999999999
------------------------------------------------------
First guess for C-H bond length:   1.0000000000000000
First guess for C-N bond length:   1.0000000000000000
------------------------------------------------------
      Iteration    RCN                          RCH                  change
          1   1.0000000000000000       1.0000000000000000       0.70619656180318990
          2   1.1693171526360502       1.6855984872546519       0.45107329962153475
          3   1.1619308212493202       1.2345856673258784       0.13531172982914874
          4   1.1572904709386174       1.0993535284743816        2.3546276314443587E-002
          5   1.1568804427643493       1.0758108224877616        5.0490108282347035E-003
          6   1.1568658506399643       1.0707618327458888        1.3471014543344922E-003
          7   1.1568650954812927       1.0694147315032179        3.7060871846898122E-004
          8   1.1568650406800285       1.0690441227888006        1.0248400700867961E-004
          9   1.1568650365173896       1.0689416387818764        2.8377157568438860E-005
         10   1.1568650361987829       1.0689132616243098        7.8602836566623653E-006
         11   1.1568650361743491       1.0689054013406531        2.1774629146439651E-006
------------------------------------------
         17   1.1568650361723185       1.0689023908752948        3.5529568176428938E-009

-------
RESULT:
-------
Bond length C-H (angstr.):   1.0689023908752948
Bond length C-N (angstr.):   1.1568650361723185

------------------------------------------------------------
Positions of nuclei (center of mass frame of reference)
------------------------------------------------------------
Set       Hydrogen                  Carbon                  Nitrogen
 1   -1.6291693581174120      -0.56026696724211722       0.59659806893020129
 2   -1.6091598235730507      -0.54025743269775583       0.61660760347456267

-----------------
Moments of inertia
-----------------
Set 1: I=   11.403991274338289      AMU angstrom**2
Set 2: I=   11.706679667685872      AMU angstrom**2

----------------------------
Derived rotational constants
----------------------------
Set 1: I=   44315.975682761506      MHz, deviation:  -1.7238496027971451E-005 MHz
Set 2: I=   43170.139983842339      MHz, deviation:  -1.6157661917759469E-005 MHz
```

Looking back on our solution, we have gained an insight into the structure determination of a rigid linear polyatomic molecule based on rotational constants of isotopomers. Owing to different nuclear masses, these isotopomers have different moments of inertia, but identical bond lengths. In fact, isotopic substitution is an often applied method in spectroscopy (see also Problem 10.6). To obtain results we had to resort to a numerical solution. It is worth drawing attention to the problems arising if more complex molecules are investigated: (1) the more complex case of nonlinear molecules is dealt with in Problem 10.5. (2) The case of polyatomic molecules with more than just three nuclear sites can indeed be tackled by systematic isotopic substitution to increase experimental data sets. This case, however, involves another problem: such molecules are more flexible, i.e., they appear in different conformations. In addition, nonrigid or *floppy* molecules

change their structure depending on their rotational state, which makes the correct interpretation of rotation or rotation-vibration spectra very puzzling.

Problem 10.5 (Asymmetric Top Rotation Spectra)
The water molecule ($H_2^{16}O$) is an asymmetric top molecule. Its bond length is $r_{OH} = 0.9584\,\text{Å}$, the angle enclosed by the OH bonds is 104.45°.

a. Determine the center of mass of the molecule, its moments of inertia, and its rotational constants A, B, and C. By convention, the rotational constants are named according to $A \geqq B \geqq C$.
b. Consider the asymmetry parameter

$$\kappa = \frac{2B - A - C}{A - C} \tag{10.55}$$

ranging from -1 to $+1$. A value of $\kappa = -1$ would indicate the limiting case of prolate symmetric top molecule; a value of $+1$, in contrast, would indicate the case of an oblate symmetric top. Calculate the asymmetry parameter for water.
c. Energy levels of the rotational states of asymmetric tops can be written in the form:

$$E(J\tau) = \frac{1}{2}(A + C)J(J + 1) + \frac{1}{2}(A - C)E_{J\tau}(\kappa) \tag{10.56}$$

where J is the rotational quantum number and $\tau = -J, \ldots, +J$ is an index. Note that in this notation energy levels are expressed in frequency units of Hertz. The function $E_{J\tau}(\kappa)$ is found in Table 10.3. Calculate the energy levels of the H_2O molecule for $J = 1, 2$. Also, calculate the energy levels of water by treating the molecule formally as an prolate or an oblate symmetric top molecule. Plot the energy levels in a term diagram. Can you explain the special labeling of asymmetric top rotator states $J_{K_aK_c}$ in Table 10.3?
d. With which axis of inertia does the permanent electric dipole moment of the H_2O molecule coincide? For transitions between pure rotational energy levels the following selection rules hold for the H_2O molecule: $\Delta J = 0, \pm 1$, $\Delta K_a = \pm 1, \pm 3$, $\Delta K_c = \mp 1, \mp 3$. Based on your results from subproblem (c), determine the possible allowed transitions and the frequency at which they occur.

Solution 10.5 This exercise deals with the rotational energy levels of symmetric and asymmetric top molecules. We familiarize ourselves with the quantum numbers involved in the description of their rotational states, and the special treatment of

Table 10.3 Algebraic relations for asymmetric rotor energy levels according to H.W. Kroto, *Molecular Rotation Spectra*, Wiley, London, 1975

$J_{K_a K_c}$	τ	$E_{J\tau}(\kappa)$
0_{00}	0	0
1_{10}	-1	$\kappa + 1$
1_{11}	0	0
1_{01}	$+1$	$\kappa - 1$
2_{20}	-2	$2\left(\kappa + \sqrt{\kappa^2 + 3}\right)$
2_{21}	-1	$\kappa + 3$
2_{11}	0	4κ
2_{12}	$+1$	$\kappa - 3$
2_{02}	$+2$	$2\left(\kappa - \sqrt{\kappa^2 + 3}\right)$

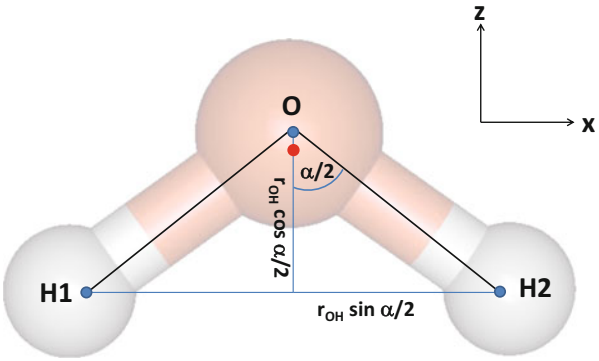

Fig. 10.9 The water molecule

asymmetric top rigid rotators. Although the rotation spectra of diatomics are quite regular, it is complicated to interpret the asymmetric top rotational spectra. The water molecule is perhaps the most prominent example of an asymmetric rotor with a well-known geometry.

In **subproblem (a)**, we determine the moments of inertia and the three rotational constants of the molecule. Given the OH bond length r_{OH} and the angle between the OH bonds α, we must first seek the center of mass. The situation is shown in Fig. 10.9. We are free to select the orientation of the molecule and tentatively place the oxygen atom in the origin at $(0, 0, 0)$. Then, the coordinates of the hydrogen atoms H1 and H2 be $\mathbf{r}_{\mathrm{H1}} = (-r_{\mathrm{OH}} \sin \frac{\alpha}{2}, 0, -r_{\mathrm{OH}} \cos \frac{\alpha}{2})$ and $\mathbf{r}_{\mathrm{H2}} = (+r_{\mathrm{OH}} \sin \frac{\alpha}{2}, 0, -r_{\mathrm{OH}} \cos \frac{\alpha}{2})$ respectively. The center of mass is generally defined

$$\mathbf{r}_{\mathrm{COM}} = \frac{\sum_i m_i \mathbf{r}_i}{\sum_i m_i} \tag{10.57}$$

where m_i are the masses of the atoms at position $\mathbf{r}_i$. The oxygen has an atomic weight of $m_O = 16$ amu; both hydrogens have a mass of 1 amu. Thus,

$$\mathbf{r}_{COM} = \frac{1}{18}\begin{pmatrix} 0 \\ 0 \\ -2r_{OH}\cos\frac{\alpha}{2} \end{pmatrix} = \frac{1}{9}\begin{pmatrix} 0 \\ 0 \\ -r_{OH}\cos\frac{\alpha}{2} \end{pmatrix} \tag{10.58}$$

The center of mass is thus 0.065 Å displaced from the oxygen center in a negative z-direction toward the hydrogens (red point in Fig. 10.9). Relative to the center of mass, the oxygen is at position $\mathbf{r}_O = \left(0, 0, \frac{1}{9}r_{OH}\cos\frac{\alpha}{2}\right)$, whereas the hydrogens take the positions $\mathbf{r}_{H1} = (-r_{OH}\sin\frac{\alpha}{2}, 0, -\frac{8}{9}r_{OH}\cos\frac{\alpha}{2})$ and $\mathbf{r}_{H2} = (+r_{OH}\sin\frac{\alpha}{2}, 0, -\frac{8}{9}r_{OH}\cos\frac{\alpha}{2})$ respectively. With these coordinates, we are ready to write down the moment of inertia tensor. The general definition is

$$\mathbf{I} = \sum_i m_i \begin{pmatrix} y_i^2 + z_i^2 & -x_i y_i & -x_i z_i \\ -y_i x_i & x_i^2 + z_i^2 & -y_i z_i \\ -z_i x_i & -z_i y_i & x_i^2 + y_i^2 \end{pmatrix} \tag{10.59}$$

As our choice of coordinates was such that the coordinate axes already coincide with the principal axes of inertia, the off-diagonal elements are all zero. The diagonal elements need to be calculated. For I_{xx} we obtain:

$$I_{xx} = 16\,\text{amu}\left(\frac{r_{OH}}{9}\cos\frac{\alpha}{2}\right)^2 + 2\,\text{amu}\left(\frac{8r_{OH}}{9}\cos\frac{\alpha}{2}\right)^2 = \left(\frac{4r_{OH}}{3}\cos\frac{\alpha}{2}\right)^2 \text{amu} \tag{10.60}$$

and thus[8] $I_{xx} = 1.0175 \times 10^{-47}\,\text{kg}\,\text{m}^2$. The second principal moment is:

$$I_{yy} = 16\,\text{amu}\left(\frac{r_{OH}}{9}\cos\frac{\alpha}{2}\right)^2 + 2\,\text{amu}\left[\left(r_{OH}\sin\frac{\alpha}{2}\right)^2 + \left(\frac{8r_{OH}}{9}\cos\frac{\alpha}{2}\right)^2\right] \tag{10.61}$$

or $I_{yy} = 2.9232 \times 10^{-47}\,\text{kg}\,\text{m}^2$. The third principal moment is:

$$I_{zz} = 2\,\text{amu}\left(r_{OH}\sin\frac{\alpha}{2}\right)^2 = 1.9059 \times 10^{-47}\,\text{kg}\,\text{m}^2. \tag{10.62}$$

With these results, we can calculate the three rotational constants:

$$A = \frac{h}{8\pi^2 I_{xx}} = 824{,}768\,\text{MHz} \tag{10.63}$$

[8] $1\,\text{amu} = 1.66054 \times 10^{-27}\,\text{kg}$.

$$B = \frac{h}{8\pi^2 I_{zz}} = 440{,}318\,\text{MHz} \tag{10.64}$$

$$C = \frac{h}{8\pi^2 I_{yy}} = 287{,}083\,\text{MHz} \tag{10.65}$$

The constants are ordered according to $A \geqq B \geqq C$. In **subproblem (b)** we determine the asymmetry parameter κ defined in Eq. (10.55). This parameter is highly useful for the interpretation of asymmetric top rotation spectra. By insertion of the values for A, B, and C we obtain a value of $\kappa = -0.4300$. In the limiting case in which two of the three moments of inertia are identical, the molecule becomes a **symmetric top** molecule. One distinguishes between more cigar-shaped *prolate* symmetric tops with $A > B = C$ and more disk-shaped *oblate* symmetric tops with $A = B > C$ respectively. The energy levels of symmetric top rigid rotators are found in the textbooks:

$$E_{JK} = \frac{\hbar^2}{2I_b} J(J+1) + K^2\hbar^2 \left(\frac{1}{2I_a} - \frac{1}{2I_b}\right) \qquad \text{prolate} \tag{10.66}$$

$$E_{JK} = \frac{\hbar^2}{2I_b} J(J+1) + K^2\hbar^2 \left(\frac{1}{2I_c} - \frac{1}{2I_b}\right) \qquad \text{oblate} \tag{10.67}$$

If the energy levels are expressed as a frequency in Hertz, these expressions simply read:

$$E_{JK} = BJ(J+1) + K^2(A-B) \qquad \text{prolate}, B = C \tag{10.68}$$

and

$$E_{JK} = BJ(J+1) + K^2(C-B) \qquad \text{prolate}, A = B \tag{10.69}$$

Compared with the treatment of the diatomic rigid rotator, a new quantum number, $K = 0, \pm 1, \ldots, \pm J$ occurs. The energy levels are degenerated because of the K^2 dependence. The wave functions for the symmetric top rotator are the *Wigner rotation functions* $D^J_{MK}(\theta, \phi, \psi)$. They are generalized spherical harmonics depending on the three *Euler angles* describing the orientation of a molecule in space [2]. Although the symmetric top rigid rotator problem can be treated exactly in a straightforward fashion, the asymmetric rotor problem is tedious, although analytic expressions for the energy levels exist. They can be found if for a given quantum number J the wave function is written as a series over all possible Wigner functions:

$$\Psi_{JM} = \sum_{K=-J}^{J} c_K D^J_{MK}. \tag{10.70}$$

The resulting expressions for $J = 0, 1, 2$ are given in the text of **subproblem (c)** (Eq. (10.56) and Table 10.3). It is our task to calculate these first rotational levels for the water molecule. Like the quantum number K in the symmetric top case, there

is an index $\tau = -J, \ldots, +J$ for the $(2J + 1)$ energy levels. The case $J = 0$ is trivial; we find $E(0, 0) = 0$. Starting with $J = 1$, we take Eq. (10.56) and pick the appropriate function $E_{1,-1}(\kappa)$ from Table 10.3. Looking at the definition of the asymmetry parameter κ we notice that simplifications are possible:

$$E(1,-1) = \frac{1}{2}(A+C)2+\frac{1}{2}(A-C)\left(\frac{2B-A-C}{(A-C)}+1\right) = A+B = 1265{,}086\,\text{MHz} \tag{10.71}$$

In a similar fashion, we obtain:

$$E(1,0) = \frac{1}{2}(A+C)2 = A+C = 1111{,}851\,\text{MHz} \tag{10.72}$$

and

$$E(1,+1) = \frac{1}{2}(A+C)2+\frac{1}{2}(A-C)\left(\frac{2B-A-C}{(A-C)}-1\right) = A+B = 727{,}401\,\text{MHz} \tag{10.73}$$

For $J = 2$, we can simplify the expressions for $\tau = -1, 0, 2$ in an analogous way and obtain:

$$E(2,-1) = 4A+B+C = 4{,}026{,}473\,\text{MHz} \tag{10.74}$$

$$E(2,0) = A+4B+C = 2{,}873{,}123\,\text{MHz} \tag{10.75}$$

$$E(2,+1) = A+B+4C = 2{,}413{,}418\,\text{MHz} \tag{10.76}$$

The cases $J = 2, \tau = \pm 2$ are more complicated. The expression from Table 10.3 is $E_{2,\pm 2}(\kappa) = 2\left(\kappa \pm \sqrt{\kappa^2+3}\right)$ and by insertion of the proper value of κ the results are $E(2,-2) = 4{,}063{,}909\,\text{MHz}$ and $E(2,+2) = 2{,}144{,}767\,\text{MHz}$. As requested, we plot all these values in a term diagram, which is depicted in Fig. 10.10 (red levels). The labeling of the various levels is in accordance with the first column of Table 10.3, in the form J_{K_a,K_c}. At first sight, this notation seems to be quite opaque. In the rest of this exercise we try to obtain a deeper understanding of this notation, which is common in the literature. Therefore, we formally treat the water molecule as a symmetric top rigid rotator and determine the energy levels. We start with the prolate case ($\kappa = -1$), in which the rotational constants B and C are identical. We use Eq. (10.68) to calculate the energy levels for $J = 0, 1, 2$ and the possible values for the quantum number K. The results are depicted in Fig. 10.10 on the left-hand side at $\kappa = -1$. Next, we consider the oblate case ($\kappa = +1$, $B = A$) and proceed in an analogous way. In the term diagram, these energy levels are shown on the right-hand side at $\kappa = +1$. A close look at the dashed lines connecting certain prolate and oblate energy levels reveals the meaning of the special labeling of asymmetric top rotator states plotted at the appropriate $\kappa = -0.43$. Consider, for example, the asymmetric top level 2_{12}. It is exactly on the intersection line between the prolate $2,\pm 1$ state and the oblate $2,\pm 2$ state. Most

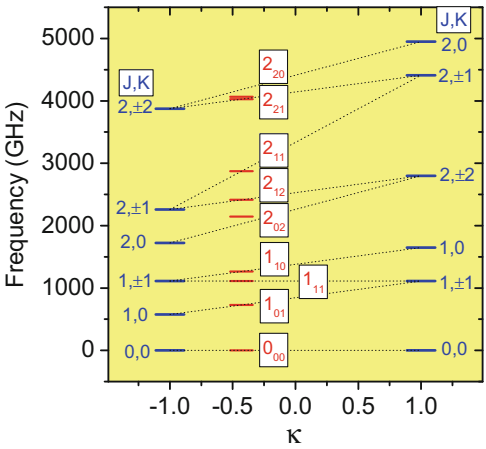

Fig. 10.10 Correlation diagram of the first $H_2^{16}O$ rotational levels (*red lines*). The special labeling of the levels is in accordance with Table 10.3. Also shown are the energy levels for water treated formally as a prolate symmetric top ($\kappa = -1$, rotational constant $B = C$), and as an oblate symmetric top ($\kappa = +1$, rotational constant $B = A$)

of the levels match with an appropriate intersection line.[9] Figure 10.10 is called a **correlation diagram**. It reveals the location of energy levels of the water molecule if the asymmetry parameter κ changes between the limiting cases -1 (prolate) to $+1$ (oblate). Although the numbers K are only quantum numbers for these limiting cases of symmetric top rotors, they are also used as projection quantum numbers in the case of an asymmetric top rotator.

The irregularity in the asymmetric top energy levels clearly complicates the rotation spectra. In **subproblem (d)**, we focus on possible transitions between the energy levels. The selection rules for asymmetric top molecules are generally complicated. They depend on the direction of the dipole moment. In our case of the H_2O molecule, the direction of the permanent dipole moment coincides with the symmetry axis of the molecule, i.e., the z-axis in Fig. 10.9. This is because the neutral molecule has a negative partial charge at the oxygen end, and a positive partial charge at the hydrogen end. As the z-axis is also the b-axis of inertia, the selection rules for so-called *b-type transitions* hold. These are:

$$\Delta J = 0, \pm 1, \quad \Delta K_a = \pm 1, \pm 3, \quad \Delta K_c = \mp 1, \mp 3 \tag{10.77}$$

where K_a is the projection quantum number on the limiting case of a prolate symmetric top, and K_b the projection quantum number on the oblate symmetric top. Transitions between $J = 0$ and $J = 1$ are apparently forbidden. Only two transitions are possible:

$$1_{10} \leftrightarrow 1_{01} : \Delta E = (12{,}365{,}086 - 727{,}401)\,\text{MHz} = 537{,}685\,\text{MHz}$$

and

$$2_{11} \leftrightarrow 2_{02} : \Delta E = (2{,}873{,}123 - 2{,}144{,}767)\,\text{MHz} = 728{,}356\,\text{MHz}$$

[9] The deviations are due to the fact that the intersection lines have a curvature.

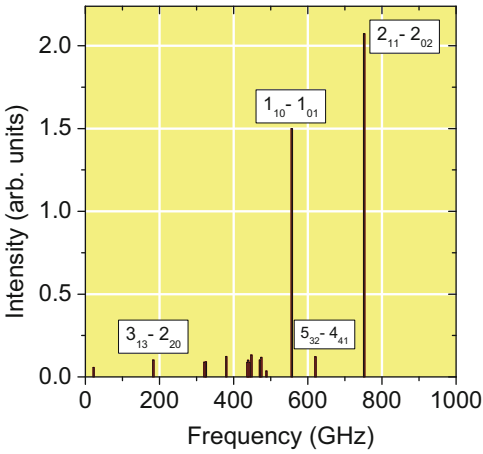

Fig. 10.11 Microwave pure rotational *stick* spectrum of $H_2^{16}O$ according to data taken from F.C. de Lucia, P. Helminger, W.H. Kirchhoff, *Microwave spectra of molecules of astrophysical interest V: water vapor*, J. Phys. Chem. Ref. Data, 2 (1974), 211

Note that because of the irregular spacing between the rotational transitions; transitions from higher excited molecules ($J > 2$) certainly agglomerate in the vicinity of these two transitions. This complicates the interpretation of microwave spectra. Useful for the assignment of transitions is the fact that states with higher J have a lower occupation probability because of the Boltzmann statistics. Therefore, transitions from these states have a lower intensity in the microwave spectrum. Such a spectrum is shown in Fig. 10.11. Note the transition with the lowest frequency at 22.2 GHz. It is the $6_{16} \leftrightarrow 5_{23}$ transition. The frequency of many kitchen microwave ovens is aligned with this transition.

Problem 10.6 (IR Spectra of Diatomics I)

a. $^1H^{35}Cl$ has an infrared transition at 2,991 cm^{-1} assigned to the stretching vibration of this diatomic molecules. For the homonuclear diatomics such as H_2 or Cl_2 no infrared active transition is observed. Why?
b. Calculate the force constant k of $^1H^{35}Cl$ in the approximation of the harmonic oscillator.
c. Calculate the wave number of the infrared transition if hydrogen is replaced by deuterium.
d. The potential between H and Cl is essentially anharmonic. A frequently used model for the anharmonic oscillator is the Morse potential

$$V(r) = D_e \left[1 - e^{-a(r-R_e)}\right]^2 \tag{10.78}$$

and the energy states of the Morse oscillator are given by:

(continued)

Problem 10.6 (continued)

$$E_n = h\nu\left(n+\frac{1}{2}\right) - \frac{(h\nu)^2}{4D_e}\left(n+\frac{1}{2}\right)^2 \tag{10.79}$$

where ν is the frequency of the stretch mode, $D_e = 7.41 \times 10^{-19}\,\mathrm{J}$ is the depth of the potential, and $R_e = 1.275\,\text{Å}$ is its minimum. For the parameter a describing the steepness of the potential the following relation holds:

$$a = \sqrt{\frac{k}{2D_e}} \tag{10.80}$$

How many vibrational states has the HCl molecule?

e. An anharmonic oscillator allows overtone transitions. Calculate the wave number of the transition $n = 0 \rightarrow 2$. At which wave number would the *hot band* $n = 1 \rightarrow 2$ be observed? On the basis of occupation probabilities, judge if the hot band is observed at $T = 300\,\mathrm{K}$.

Solution 10.6 Hydrogen chloride (Fig. 10.12) is a heteronuclear diatomic molecule. Chlorine is more electronegative and causes an accumulation of electronic charge density δ^- at its atomic site, and a depletion of charge density at the hydrogen site. This causes a static electric dipole moment of the molecule and, in addition, a **polar bond**. For this reason, a harmonic variation of the bond length causes an **induced electric dipole moment** which may couple to the oscillating electric field of an electromagnetic wave. As a consequence, the H-Cl stretch mode is infrared active and the transition is observed at $\tilde{\nu} = 2991\,\mathrm{cm}^{-1}$.

In **subproblem (a)**, we explain why analogous transitions are not observed for the homonuclear diatomics H_2 and Cl_2. For symmetry reasons, it is obvious that these molecules do not carry partial charges at their atomic sites and their atomic bonds are not polar. Therefore, no induced dipole moment is involved with the harmonic variation of their bond lengths. Hence, their stretch modes do not couple to the external electrical field of an electromagnetic wave and these modes are infrared inactive.

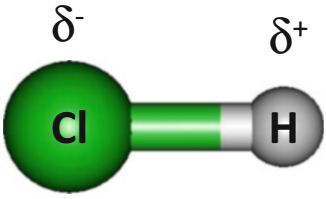

Fig. 10.12 The heteronuclear diatomic HCl

In **subproblem (b)**, we treat the stretching mode of the HCl molecule within the approximation of the harmonic oscillator and calculate the force constant k associated with the bond. Using Eq. (10.16), the force constant is:

$$k = \mu\,(2\pi\nu)^2 = \mu\,(2\pi\tilde{\nu}c)^2 \tag{10.81}$$

For the HCl molecule, the effective mass is thus:

$$\mu_{\mathrm{HCl}} = \frac{\mu_{\mathrm{H}}\mu_{\mathrm{Cl}}}{\mu_{\mathrm{H}} + \mu_{\mathrm{Cl}}} = \frac{35}{36} \times 1.66054 \times 10^{-27}\,\mathrm{kg} = 1.61441 \times 10^{-27}\,\mathrm{kg}. \tag{10.82}$$

Hence, the force constant sought is

$$\begin{aligned} k &= 1.61441 \times 10^{-27}\,\mathrm{kg}\left(2\pi \times 2991\,\mathrm{cm}^{-1} \times 2.997925 \times 10^{10}\,\mathrm{cm\,s}^{-1}\right)^2 \\ &= 512.4424\,\mathrm{kg\,s}^{-2} \approx 512\,\mathrm{N\,m}^{-1}. \end{aligned}$$

The wave number of a vibrational transition depends on the effective mass. It is common practice in vibrational spectroscopy to change the isotopes of certain atomic species to obtain additional information about the molecular structure and dynamics.

In **subproblem (c)**, we determine the wave number of the stretch vibration if hydrogen is replaced by deuterium. Note that this does not notably change the electronic structure of the molecule. Thus, the value of the force constant k is not affected by this replacement. Again using Eq. (10.16), we can write:

$$\frac{\nu_{\mathrm{DCl}}}{\nu_{\mathrm{HCl}}} = \sqrt{\frac{\mu_{\mathrm{HCl}}}{\mu_{\mathrm{DCl}}}} \tag{10.83}$$

The effective mass for DCl is (Eq. (10.82)) $\mu_{\mathrm{DCl}} = \frac{2\times35}{37} m_u$. Taking the effective masses for both isotopomers and the relation between frequency and wave number ($\tilde{\nu} = \frac{\nu}{c}$), we obtain:

$$\frac{\tilde{\nu}_{\mathrm{DCl}}}{\tilde{\nu}_{\mathrm{HCl}}} = 0.717 \tag{10.84}$$

Thus, the stretch mode of DCl is expected at:

$$\tilde{\nu}_{\mathrm{DCl}} = 0.717 \times 2991\,\mathrm{cm}^{-1} = 2145\,\mathrm{cm}^{-1}.$$

In **subproblem (d)**, we take anharmonicity into account and deal with the number of vibrational states in the HCl molecule. When reading the problem text for the first time we get stuck and ask ourselves what this means: the *number* of vibrational states. We must be aware that, depending on the shape of the potential, a quantum system may have a finite number of discrete bound states. Although for example

the particle in a box with infinite walls and also the harmonic oscillator have an infinite number of discrete states, a particle in a finite potential well is an example of a system that has only a finite number of discrete states. For energies exceeding the potential well depth, the energy spectrum becomes continuous and the particle may leave the box. Extrapolated to the case of a vibrating diatomic molecule with an interatomic potential allowing for dissociation, the number of bound states should be finite. A simple and frequently used model for the anharmonic potential between two atomic sites is the Morse potential Eq. (10.78). It has only three parameters a, D_e, and R_e, and it has the advantage that the energy levels are well-defined (Eq. (10.79)):

$$E_n = h\nu\left(n + \frac{1}{2}\right) - \frac{(h\nu)^2}{4D_e}\left(n + \frac{1}{2}\right)^2$$

The first term is identical to the harmonic oscillator expression for the energy in state n. The second term can be interpreted as a correction resulting from anharmonicity. The minus sign is important, i.e., the correction leads to shrinking of the energy differences between adjacent states. The situation is illustrated in Fig. 10.13, where the potential is plotted with the given values for the potential depth D_e, the potential minimum R_e, and the parameter a describing the steepness of the potential,

$$a = \sqrt{\frac{k}{2D_e}} = 1.85951 \times 10^{10}\,\mathrm{m}^{-1}. \tag{10.85}$$

Also shown are the energy levels resulting from Eq. (10.79) and the quantum energy $h\nu = h\tilde{\nu}c = 5.9414 \times 10^{-20}\,J = 0.37\,\mathrm{eV}$. In Fig. 10.14, the energies E_n are plotted against the quantum number n. As the dissociation energy is gradually reached, the energy levels are expected to approach one another, which is indeed the

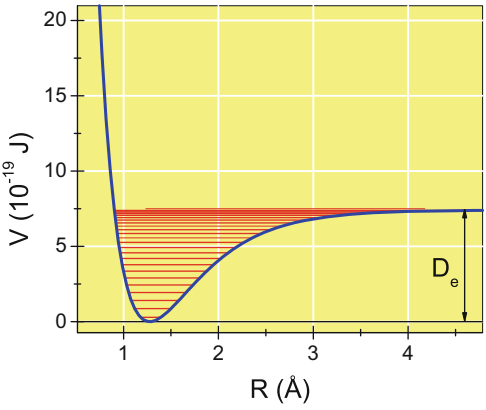

Fig. 10.13 The anharmonic potential in the HCl molecule, based on the Morse oscillator model. Also shown are the resulting energy levels of the Morse oscillator

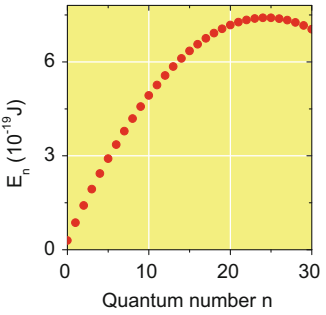

Fig. 10.14 Vibrational energies of the HCl molecule as a function of quantum number n, calculated with Eq. (10.79). Realistic energy levels are those between $n = 0$ and 24

case for quantum numbers up to $n = 24$. For $n > 24$, however, Eq. (10.79) predicts that E_n become smaller with increasing n. This is unphysical. Therefore, the number of vibrational states of the HCl molecule is 25 ($n = 0$–24).

As we have seen, one consequence of anharmonicity is the shift in the energy levels. The energies of the first levels are

$$E_0 = \frac{h\nu}{2} - \frac{(h\nu)^2}{4D_e}\frac{1}{4} = 0.29410 \times 10^{-20}\,\mathrm{J} \tag{10.86}$$

$$E_1 = \frac{h\nu}{2}3 - \frac{(h\nu)^2}{4D_e}\frac{9}{4} = 8.64420 \times 10^{-20}\,\mathrm{J} \tag{10.87}$$

$$E_2 = \frac{h\nu}{2}5 - \frac{(h\nu)^2}{4D_e}\frac{25}{4} = 1.41092 \times 10^{-19}\,\mathrm{J} \tag{10.88}$$

Therefore, the fundamental $n = 0 \rightarrow 1$ transition is observed at:

$$\tilde{\nu}_{0\rightarrow 1} = \frac{\Delta E_{0\rightarrow 1}}{hc} = 2871\,\mathrm{cm}^{-1} \tag{10.89}$$

which means a red-shift of $120\,\mathrm{cm}^{-1}$, in comparison with the pure harmonic wave number. The transition is shown in Fig. 10.15 in another term scheme of the first few vibrational levels. Also shown in this figure are additional transitions that we deal with in **subproblem (e)**. A consequence of anharmonicity is the breaking of selection rules of the harmonic oscillator. Therefore, the overtone transition $n = 0 \rightarrow 2$ is no longer forbidden. Taking the energy difference between the levels $n = 2$ and the ground state we find:

$$\tilde{\nu}_{0\rightarrow 2} = \frac{\Delta E_{0\rightarrow 2}}{hc} = 5623\,\mathrm{cm}^{-1}. \tag{10.90}$$

Note that overtone transitions and combination bands are always much less intense than the corresponding fundamentals. **Hot bands** are another type of IR transitions. In absorption spectroscopy, they result from the excitation of a molecule

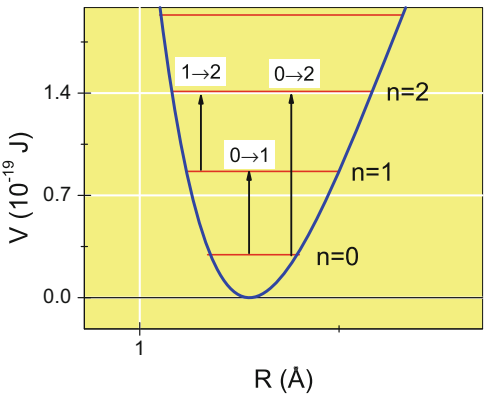

Fig. 10.15 Term scheme and vibrational excitations in the region of the first excited states of the HCl molecule

in an excited vibrational state. In our case, we consider the transition $n = 1 \rightarrow 2$. By taking the difference in energy between these two states we obtain:

$$\tilde{\nu}_{1\rightarrow 2} = \frac{\Delta E_{1\rightarrow 2}}{hc} = 2752\,\mathrm{cm}^{-1}. \tag{10.91}$$

We further investigate whether this transition should be observable under room temperature conditions using occupation probabilities. What is behind it? The transition $n = 1 \rightarrow 2$ is only observable if the state $n = 1$ is notably occupied. The occupation probability p_n for a state n follows the Boltzmann statistics:

$$p_n = \frac{\exp\left(-\frac{E_n}{k_B T}\right)}{\sum_n \exp\left(-\frac{E_n}{k_B T}\right)} \tag{10.92}$$

At room temperature, the thermal energy ($k_B T \approx 4 \times 10^{-21}\,\mathrm{J}$) is considerably lower than the vibrational quantum energy.[10] It is therefore justified to consider only the first few vibrational levels. At room temperature ($T = 300\,\mathrm{K}$), we obtain the following occupation probability for $n = 1$:

$$p_1 \approx \frac{\exp\left(-\frac{E_1}{k_B T}\right)}{\exp\left(-\frac{E_0}{k_B T}\right) + \exp\left(-\frac{E_1}{k_B T}\right) + \exp\left(-\frac{E_2}{k_B T}\right)} = 1.05 \times 10^{-6}.$$

A similar calculation for the ground state would show $p_0 \approx 0.999999$. Thus, the level $n = 1$ has negligible occupation probability. At room temperature, therefore, the hot band transition $n = 1 \rightarrow 2$ is not detectable using usual laboratory spectrometer hardware. The variation of occupation probabilities with temperature

[10] See also Problem 10.1b.

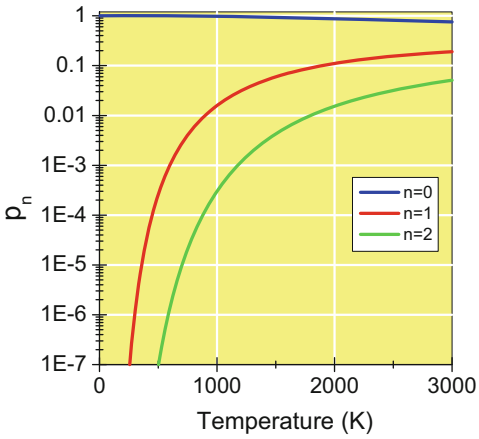

Fig. 10.16 Occupation probabilities of the ground state and the first excited vibrational states of the HCl molecule according to Boltzmann statistics

is shown in Fig. 10.16 for the ground state and the first two excited states. At 1,000 K the probability of the first excited state reaches a value of about 1%. Are hot bands thus relevant at all for room temperature experiments? An inspection of the IR spectrum of the greenhouse gas CO_2, for example, reveals a hot band in the region of its asymmetric bending mode ($\tilde{\nu} \approx 673\,\mathrm{cm}^{-1}$). The spectra of other polyatomic molecules such as SF_6, another greenhouse gas, are also complicated by hot bands.

Problem 10.7 (IR Spectra of Diatomics II)
In high resolution IR spectroscopy experiments, the fundamental stretch mode and the first overtone of the diatomic CO was investigated. The measured IR transitions are given in Table 10.4.

a. The energy levels of the perturbed rotation-vibration energy are:

$$E_{nJ} = V(R_e) + h\nu_e\left(n+\frac{1}{2}\right) + hB_eJ(J+1) - h\nu_e x_e\left(n+\frac{1}{2}\right)^2 - h\alpha_e\left(n+\frac{1}{2}\right)J(J+1) - h\bar{D}_eJ^2(J+1)^2 \tag{10.93}$$

where $V(R_e)$ is the potential at the equilibrium bond length R_e, ν_e is the harmonic frequency of the stretch vibration, x_e the anharmonicity constant, α_e is the rotation vibration coupling constant, $\bar{D}_e$ is the centrifugal distortion constant. Determine $B_e, \alpha_e, R_e, x_e, \bar{D}_e$ from a suitable polynomial fit of the spectroscopic data. *Hint: Write down relations for the transition*

(continued)

Problem 10.7 (continued)
frequencies of the fundamental and first overtone. Introduce new parameters $J' = J + 1$ and $m = -J'$ (P-branch), $m = J'$ (R-branch).

b. The centrifugal distortion constant is related to the rotational constant B_e via

$$\bar{D}_e = \frac{4B_e^3}{\nu_e^2}. \tag{10.94}$$

Does the fitted result for $\bar{D}_e$ satisfy this condition?

c. Use relations provided in Problem 10.6 to set up a Morse potential model for the CO molecule. Determine the bond dissociation energy for the CO molecule.

d. The vibrational Hamiltonian of a diatomic including anharmonic corrections can be written:

$$H_{\text{vib}} = H_{\text{harmonic}} + \frac{1}{3!}\left(\frac{\partial^3 V}{\partial q^3}\right)_e q^3 + \frac{1}{4!}\left(\frac{\partial^4 V}{\partial q^4}\right)_e q^4 + \cdots \tag{10.95}$$

where q is the elongation $r - R_e$ and $\left(\frac{\partial^3 V}{\partial q^3}\right)_e$ and $\left(\frac{\partial^4 V}{\partial q^4}\right)_e$ are the cubic and quartic force constants respectively. The latter are related to experimentally accessible quantities by means of:

$$\alpha_e = \frac{-2B_e^2}{\nu_e}\left[\frac{2B_e R_e^3\left(\frac{\partial^3 V}{\partial q^3}\right)_e}{h\nu_e^2} + 3\right] \tag{10.96}$$

and

$$x_e\nu_e = \frac{B_e^2 R_e^4}{4h\nu_e^2}\left[\frac{10B_e R_e^2\left(\frac{\partial^3 V}{\partial q^3}\right)_e^2}{3h\nu_e^2} - \left(\frac{\partial^4 V}{\partial q^4}\right)_e\right] \tag{10.97}$$

Determine the cubic and quartic force constants and compare the resulting anharmonic potential model with the Morse potential model from subproblem (c).

Solution 10.7 With this challenging exercise, we explore the foundations of molecular spectroscopy beyond the rigid rotator-harmonic oscillator (RRHO) approximation. In Problem 10.4 we have determined bond lengths of a molecule from the rotational constants obtained from pure rotation spectra. In the discussion of the

Table 10.4 Measured wave numbers of gas-phase rovibrational transitions of carbon monoxide

	$n = 0 \rightarrow 1$		$n = 0 \rightarrow 2$	
J	P	R	P	R
0	2, 139.427	2, 147.082	4, 256.216	4, 263.837
1	2, 135.547	2, 150.856	4, 252.301	4, 267.542
2	2, 131.632	2, 154.596	4, 248.317	4, 271.177
3	2, 127.683	2, 158.300	4, 244.262	4, 274.740
4	2, 123.700	2, 161.969	4, 240.138	4, 278.234
5	2, 119.681	2, 165.601	4, 235.947	4, 281.656
6	2, 115.629	2, 169.198	4, 231.685	4, 285.009
7	2, 111.544	2, 172.759	4, 227.354	4, 288.289
8	2, 107.423	2, 176.284	4, 222.954	4, 291.499
9	2, 103.270	2, 179.772	4, 218.486	4, 294.638
10	2, 099.083	2, 183.224	4, 213.949	4, 297.704
11	2, 094.863	2, 186.639	4, 209.343	4, 300.700
12	2, 090.609	2, 190.018	4, 204.668	4, 303.623
13	2, 086.322	2, 193.360	4, 199.929	4, 306.475
14	2, 082.003	2, 196.664	4, 195.117	4, 309.254
15	2, 077.650	2, 199.931	4, 190.239	4, 311.961
16	2, 073.265	2, 203.161	4, 185.295	4, 314.596
17	2, 068.847	2, 206.354	4, 180.282	4, 317.159
18	2, 064.397	2, 209.509	4, 175.203	4, 319.649
19	2, 059.915	2, 212.626	4, 170.055	4, 322.064
20	2, 055.401	2, 215.705	4, 164.839	4, 324.409
21	2, 050.855	2, 218.746	4, 159.560	4, 326.681
22	2, 046.276	2, 221.749	4, 154.212	4, 328.878
23	2, 041.667	2, 224.713	4, 148.797	4, 331.004
24	2, 037.026	2, 227.639		4, 333.053
25		2, 230.526		4, 335.030
26		2, 233.375		
27		2, 236.185		

All values in cm^{-1}. J is the rotational quantum number of the final state for the P-branch ($J+1 \rightarrow J$), and of the initial state for the R-branch ($J \rightarrow J+1$) respectively

results it was mentioned that even in the vibrational ground state, the rotational constants are slightly influenced by vibration rotation coupling. Neglect of such effects involves a slight systematic error in the determination of bond lengths. In this problem, we focus on such effects in detail and treat vibration and rotation all together. In gas-phase infrared absorption spectra, vibrational transitions go along with changes in the rotational state. The selection rules for a diatomic rotor, $\Delta J = \pm 1$ (see Eq. (10.15)), lead to a regular wing-like arrangement of the vibration rotation transitions as shown in Fig. 10.17 for the first overtone vibration. The experimental line positions are given in Table 10.4. The P-branch results from transitions $n, J+1 \rightarrow n+1, J$, the R-branch from the transitions $n, J \rightarrow n+1, J+1$

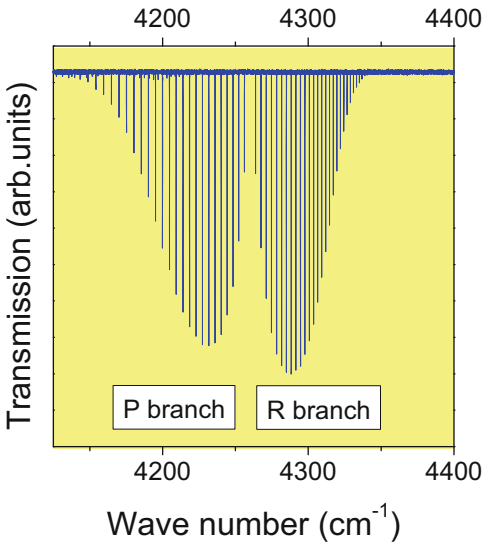

Fig. 10.17 Rotationally resolved IR spectrum in the region of the first overtone ($0 \rightarrow 2$) of the $^{12}C^{16}O$ stretch vibration

respectively. J is the usual rotational quantum number. The Q-branch $n, J \rightarrow n+1, J$ is left out.[11] In **subproblem (a)**, we use these data to determine spectroscopic constants included in Eq. (10.93). It is useful to analyze this equation, which is the result of a tedious perturbation treatment of the rigid-rotator harmonic-oscillator (RRHO) model, in detail. The first three terms are the vibration-rotation energy of the unperturbed RRHO model. The following three terms are the first corrections from the perturbation treatment, which typically lead to a decrease in the energy levels. Anharmonicity—the first correction term—has already been introduced in Problem 10.6. The second correction is the rotation vibration coupling, whereas the last correction stems from the centrifugal distortion of the molecule depending on its rotational state. For the comparison with the experimental data we must set up expressions for the transition frequencies in the fundamental and overtone region. We start with writing down the energies for the ground and the first vibrationally excited state. Following the hints given, we introduce the new parameter $J' = J+1$:

$$E_{0,J} = \frac{h\nu_e}{2} - \frac{h\nu_e x_e}{4} + hB_0(J'-1)J' - h\bar{D}_e(J'-1)^2J'^2 \tag{10.98}$$

$$E_{0,J+1} = \frac{h\nu_e}{2} - \frac{h\nu_e x_e}{4} + hB_0J'(J'+1) - h\bar{D}_eJ'^2(J'+1)^2 \tag{10.99}$$

[11] The Q-branch would require $\Delta J = 0$ which is forbidden. Infrared active modes of polyatomic molecules, however, have a Q-branch if the induced electric dipole moment is oriented perpendicular to the symmetry axis of a molecule. A Q-branch is also observed in the vibration rotation spectrum of the paramagnetic NO molecule.

$$E_{1,J} = \frac{3h\nu_e}{2} - \frac{9h\nu_e x_e}{4} + hB_1(J'-1)J' - h\bar{D}_e(J'-1)^2J'^2 \tag{10.100}$$

$$E_{1,J+1} = \frac{3h\nu_e}{2} - \frac{9h\nu_e x_e}{4} + hB_1J'(J'+1) - h\bar{D}_eJ'^2(J'+1)^2 \tag{10.101}$$

Moreover, we have introduced the vibrationally corrected rotational constants

$$\begin{aligned} B_0 &= B_e - \frac{\alpha_e}{2} \\ B_1 &= B_e - \frac{3\alpha_e}{2}. \end{aligned} \tag{10.102}$$

Before we consider energy differences, this auxiliary calculation is useful:

$$\begin{aligned} J'^2(J'+1)^2 &= J'^2(J'^2+2J'+1) = J'^4 + 2J'^3 + J'^2 \\ (J'-1)^2J'^2 &= (J'^2-2J'+1)J'^2 = J'^4 - 2J'^3 + J'^2 \end{aligned}$$

If we consider the difference between these two expressions, all terms but the cubic ones cancel each other out. As a consequence, we can form the transition frequencies for the P-branch of the fundamental lines:

$$\text{P:}\Delta\nu_{0,J+1\to1,J} = \frac{E_{1,J} - E_{0,J+1}}{h} = \nu_e - 2\nu_e x_e - (B_1+B_0)J' + (B_1-B_0)J'^2 + 4\bar{D}_eJ'^3 \tag{10.103}$$

$$\text{R:}\Delta\nu_{0,J\to1,J+1} = \frac{E_{1,J+1} - E_{0,J}}{h} = \nu_e - 2\nu_e x_e + (B_1+B_0)J' + (B_1-B_0)J'^2 - 4\bar{D}_eJ'^3 \tag{10.104}$$

Inspection of these expressions reveals that they can be combined if we introduce the new parameter $m = -J'$ for the P-branch and $m = J'$ for the R-branch. Then, the transition frequencies for the region $n = 0 \to 1$ are:

$$\Delta\nu_m = \nu_e - 2\nu_e x_e + (B_1+B_0)m + (B_1-B_0)m^2 - 4\bar{D}_em^3 \tag{10.105}$$

The corresponding wave numbers are obtained after division by the speed of light, $c = 2.99792458 \times 10^{10}\,\text{cm}\,\text{s}^{-1}$. If we plot the transition wave numbers against m, we obtain a curved line. Such a plot is shown in Fig. 10.18. A cubic fit of the form:

$$\Delta\tilde{\nu}(m) = a_0 + a_1m + a_2m^2 + a_3m^3 \tag{10.106}$$

with these data provide the values of $\nu_e(1-2x_e)$, B_1+B_0, B_1-B_0, and $\bar{D}_e$. The result of the cubic fit is shown in Table 10.5. Before we further evaluate these results, we must first consider the transitions of the first overtone.

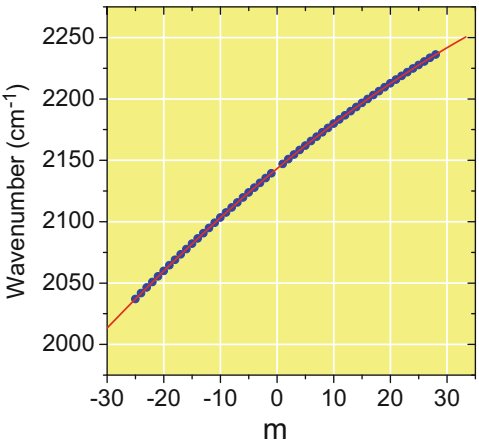

Fig. 10.18 Polynomial plot of the experimental data of rovibrational transitions in the region $n = 0 \rightarrow 1$. For the definition of the parameter m, see the text of subproblem (a)

Table 10.5 Results of the polynomial fit of the experimental data put into graphs in Fig. 10.18 and in Fig. 10.19

Vib. transition	a_0	a_1	a_2	a_3
$0 \rightarrow 1$	2143.27144(7)	3.82754(1)	−0.0175	$-2.443(2) \times 10^{-5}$
$0 \rightarrow 2$	4260.0617(2)	3.81006(2)	−0.035	$-2.449(4) \times 10^{-5}$

The coefficients a_i, $i = 0, \ldots, 4$ are defined in Eq. (10.106). Numbers in parentheses give the statistical uncertainty in units of the last significant digit. All values are in units of cm^{-1}

The treatment is very similar. After introduction of a vibrationally corrected rotational constant $B_2 = B_e - \frac{5\alpha_e}{2}$ we obtain the expressions

$$\mathrm{P}{:}\Delta\nu_{0,J+1\rightarrow 2,J} = \frac{E_{2,J} - E_{0,J+1}}{h} = 2\nu_e - 6\nu_e x_e - (B_2 + B_0)\,J' + (B_2 - B_0)\,J'^2 + 4\bar{D}_e J'^3 \tag{10.107}$$

$$\mathrm{R}{:}\Delta\nu_{0,J\rightarrow 2,J+1} = \frac{E_{2,J+1} - E_{0,J}}{h} = 2\nu_e - 6\nu_e x_e + (B_2 + B_0)\,J' + (B_2 - B_0)\,J'^2 - 4\bar{D}_e J'^3 \tag{10.108}$$

which can be combined to form:

$$\Delta\nu_m = 2\nu_e - 6\nu_e x_e + (B_2 + B_0)\,m + (B_2 - B_0)\,m^2 - 4\bar{D}_e m^3. \tag{10.109}$$

A plot of the data of the overtone region against m is shown in Fig. 10.19. The results of the polynomial fit are shown in Table 10.5.

We are now ready to exploit the data in Table 10.5 to obtain the quantities sought. First, we focus on the coefficients a_0 containing the harmonic wave number and the anharmonicity constant. From

$$a_0^{0\rightarrow 1} = \tilde{\nu}_e - 2\tilde{\nu}_e x_e$$

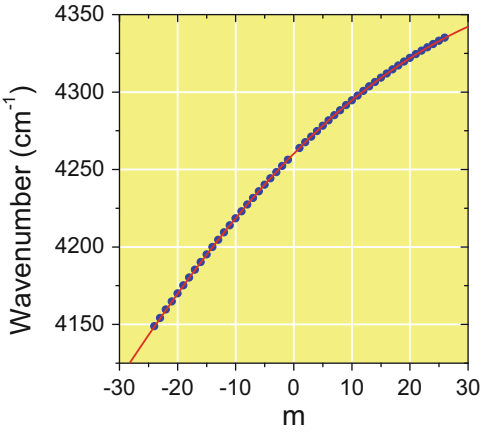

Fig. 10.19 Polynomial plot of the experimental data of rovibrational transitions in the region $n = 0 \rightarrow 2$. For the definition of the parameter m, see the text of subproblem (a):

$$a_0^{0\rightarrow 2} = 2\tilde{\nu}_e - 6\tilde{\nu}_e x_e$$

we obtain

$$\tilde{\nu}_e = 3a_0^{0\rightarrow 1} - a_0^{0\rightarrow 2} = 2169.7526(1)\,\mathrm{cm}^{-1} \tag{10.110}$$

and

$$x_e = \frac{2a_0^{0\rightarrow 1} - a_0^{0\rightarrow 2}}{2\tilde{\nu}_e} = 6.1024 \times 10^{-3}. \tag{10.111}$$

Focusing on the coefficients a_1 and a_2, we can determine the rotational constants. Because

$$a_1^{0\rightarrow 1} = \frac{1}{c}\,(B_1 + B_0)$$
$$a_2^{0\rightarrow 1} = \frac{1}{c}\,(B_1 - B_0)\,,$$

we obtain[12]

$$\frac{B_1}{c} = \frac{a_1^{0\rightarrow 1} + a_2^{0\rightarrow 1}}{2} = 1.90502(1)\,\mathrm{cm}^{-1}. \tag{10.112}$$

[12]Values of rotational constants obtained from infrared spectroscopy are often presented in units of cm^{-1}. The numbers in brackets indicate the error of the fit in units of the last significant digit.

and

$$\frac{B_0}{c} = \frac{a_1^{0\to1} - a_2^{0\to1}}{2} = 1.92252(1)\,\mathrm{cm}^{-1}. \tag{10.113}$$

In frequency units, we thus obtain $B_1 = 57{,}111.1(3)\,\mathrm{MHz}$ and $B_0 = 57{,}635.7(3)\,\mathrm{MHz}$. The difference in the rotational constants is the vibration-rotation constant α_e:

$$\alpha_e = B_0 - B_1 = 524.6(6)\,\mathrm{MHz}. \tag{10.114}$$

The equilibrium rotational constant B_e follows from (Eq. (10.102))

$$\frac{B_e}{c} = \frac{B_0}{c} + \frac{\alpha_e}{2c} = 1.93127(2)\,\mathrm{cm}^{-1}. \tag{10.115}$$

or $B_e = 57898.0(6)\,\mathrm{MHz}$. Having obtained the rotational constants, we can determine the C-O bond length. The effective mass for the CO rotor is:

$$\mu = \frac{m_\mathrm{C} m_\mathrm{O}}{m_\mathrm{C} + m_\mathrm{O}} = 6.8571\,\mathrm{amu} = 1.138655 \times 10^{-26}\,\mathrm{kg}. \tag{10.116}$$

The relation between the rotational constant and the moment of inertia I or the bond length R_e is

$$B_e = \frac{h}{8\pi^2 I} = \frac{h}{8\pi^2 \mu R_e^2} \tag{10.117}$$

and thus

$$R_e = \sqrt{\frac{h}{8\pi^2 \mu B_e}} = 1.1282 \times 10^{-10}\,\mathrm{m} \tag{10.118}$$

or 1.1282 Å. For comparison, the bond length R_0 evaluated with the rotational constant in the vibrational ground state, B_0, is 1.131 Å. Finally, we determine the centrifugal distortion constant contained in the parameter a_3. The results from the two data sets are similar. From the data set of the $0 \to 1$ transitions, we obtain $\bar{D}_e = -\frac{a_3^{0\to1}}{4} = 0.183098\,\mathrm{MHz}$. From the overtone transitions, $\bar{D}_e = -\frac{a_3^{0\to2}}{4} = 0.183548\,\mathrm{MHz}$ results. Hence, a value of $0.1833(2)\,\mathrm{MHz}$ for $\bar{D}_e$ is consistent with the data. The value for the centrifugal distortion constant is further scrutinized in **subproblem (b)**. According to Eq. (10.94) it can be related to B_e. This alternative way of computing $\bar{D}_e$ is another test of the integrity of the data sets. With $\nu_e = c\tilde{\nu}_e = 65.04755 \times 10^6\,\mathrm{MHz}$ the centrifugal distortion constant is

$$\bar{D}_e = \frac{4B_e^3}{\nu_e^2} = 0.18348\,\mathrm{MHz}.$$

This value is in good agreement with the result from subproblem (a) and the condition Eq. (10.94) is reflected by the data.

Starting with **subproblem (c)** we focus on the anharmonic potential between the carbon and the oxygen core. The Morse potential model was introduced in Problem 10.6 and we apply it here once more. Comparison of Eq. (10.79) with Eq. (10.93) reveals the relationship between the anharmonicity constant x_e and the depth of the Morse potential, D_e:

$$\begin{aligned} D_e = \frac{h\nu_e}{4x_e} &= \frac{6.62606957 \times 10^{-34}\,\mathrm{J\,s} \times 6.504755 \times 10^{13}\,\mathrm{s}^{-1}}{4 \times 6.1024 \times 10^{-3}} \\ &= 1.7657 \times 10^{-18}\,\mathrm{J} = 11.02\,\mathrm{eV} \end{aligned} \tag{10.119}$$

In the Morse oscillator model, the bond dissociation energy D_0 of CO is the difference between D_e and the zero point vibration energy, $E_{n=0,J=0}$, which can be calculated according to Eq. (10.93):

$$E_{n=0,J=0} = h\nu_e \left(\frac{1}{2} - \frac{x_e}{4}\right) = 0.13\,\mathrm{eV}.$$

Hence,

$$D_0 = D_e - E_{n=0,J=0} = 10.89\,\mathrm{eV}. \tag{10.120}$$

The force constant k is calculated using Eq. (10.16):

$$\begin{aligned} k = \mu(2\pi\nu_e)^2 &= 1.138655 \times 10^{-26}\,\mathrm{kg}(2\pi \times 6.504755 \times 10^{13}\,\mathrm{s}^{-1})^2 \\ &= 1902.014\,\mathrm{N\,m}^{-1}. \end{aligned} \tag{10.121}$$

The Morse parameter a follows from Eq. (10.80):

$$a = \sqrt{\frac{k}{2D_e}} = 2.321 \times 10^{10}\,\mathrm{m}^{-1} = 2.321\,\mathrm{\AA}^{-1} \tag{10.122}$$

The third parameter is simply the equilibrium distance $R_e = 1.1282\,\mathrm{\AA}$. A plot of the Morse potential for CO is depicted in Fig. 10.20. A second way of analyzing the anharmonic potential in the CO molecule is to consider cubic and quartic force constants. They are related to the spectroscopic parameters that we have already determined in subproblem (a). We rearrange Eqs. (10.96) and (10.97) in **subproblem (d)**:

$$V^{(3)} = \left(\frac{\partial^3 V}{\partial q^3}\right)_e = -\frac{h\nu_e^2}{2B_e R_e^3}\left[3 + \frac{\nu_e \alpha_e}{2B_e^2}\right] = -1.36397 \times 10^{14}\,\mathrm{J\,m}^{-3} \tag{10.123}$$

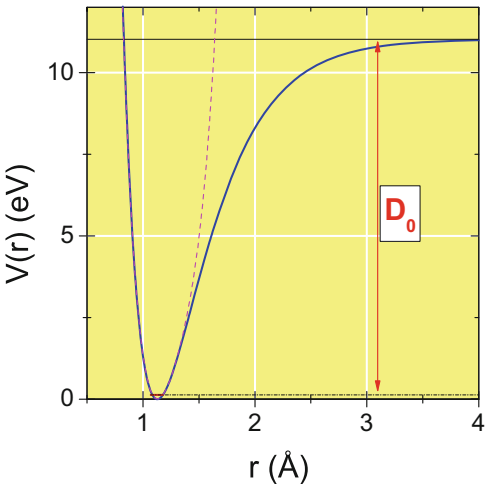

Fig. 10.20 Modeling of the potential between carbon and oxygen. The *solid line* is the Morse potential derived from spectroscopic constants. The *dashed line* is the anharmonic potential derived from the cubic and quartic force constants

The quartic force constant is:

$$V^{(4)} = \left(\frac{\partial^4 V}{\partial q^4}\right)_e = \frac{10B_eR_e^2}{3h\nu_e^2}\left(\frac{\partial^3 V}{\partial q^3}\right)_e^2 - \frac{4h\nu_e^2}{B_e^2R_e^4}x_e\nu_e = 8.1040 \times 10^{24}\,\mathrm{J\,m^{-4}} \tag{10.124}$$

With these anharmonic force constants the carbon-oxygen potential

$$V(r) = -\frac{1}{2}k(r-R_e)^2 + \frac{1}{3!}V^{(3)}(r-R_e)^3 + \frac{1}{24!}V^{(4)}(r-R_e)^4 \tag{10.125}$$

takes the form shown as the dashed line in Fig. 10.20. For $r < R_e$, the potential is very close to the Morse potential. For $r > R_e$, however, the potentials are in line only up to about a bond length of 1.5 Å. Larger elongations are not adequately described by the cubic and quartic force constants. Higher order force constants would be needed to describe such situations. Looking back on the exercise, we have learned how to cope with larger sets of spectroscopic data and how the fundamental molecular properties such as the bond length and the bond dissociation energy can be extracted from these data. Doing so we went beyond the models of the rigid rotator and the harmonic oscillator.

Problem 10.8 (Vibrational Modes of Polyatomic Molecules)
Consider the formaldehyde molecule H_2CO shown in Fig. 10.21.

a. Write down the point symmetry elements of the molecule. To which point group does this molecule belong?

(continued)

Problem 10.8 (continued)
b. How many vibrational degrees of freedom does the molecule possess?
c. Use group theory to find the symmetry types of the normal modes.
d. Which of the normal modes are infrared active, which are Raman active?

Solution 10.8 In this problem, we deal with normal modes of polyatomic molecules. The concrete example is the formaldehyde molecule H_2CO. Many problems in molecular spectroscopy are significantly simplified if symmetry considerations and group theory are used to describe molecular properties. Here, we use formaldehyde as a simple and instructive case that may be a topic in both written and oral examinations.

Starting with **subproblem (a)**, we enumerate the point symmetry elements of the molecule. A point symmetry operation transforms a molecule in such a way that the result of the transformation cannot be distinguished from the initial state. First, every molecule has at least one point symmetry element, the **identity**, which is often forgotten; therefore, we mention it first. The symmetry operation involved with the identity is the operator $\hat{E}$. Then, the molecule has a twofold **rotation axis**; the operation is $\hat{C}_2$. Further point symmetry elements are **vertical mirror planes**, the xz-plane and the yz-plane. The operators are $\hat{\sigma}_v(xz)$ and $\hat{\sigma}'_v(yz)$. The point symmetry elements (except for the identity) are shown in Fig. 10.22. Almost certainly, when molecular symmetry was introduced in your chemistry lectures, it was done using the water molecule as an instructive example. If we compare formaldehyde with water, we see that they share the same point symmetry elements.[13] Like the H_2O molecule, formaldehyde has the point group C_{2v}.

In **subproblem (b)** we determine the number of vibrational degrees of freedom. The molecule has $N = 4$ nuclei, and each of the nuclei has three translational degrees of freedom. Hence, the molecule has $3N = 12$ degrees of freedom. To obtain the number of vibrational degrees of freedom, we subtract the three pure translational degrees of freedom of the molecule's center of mass. Moreover,

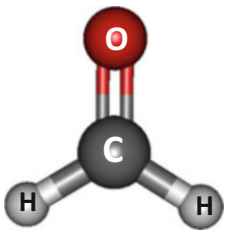

Fig. 10.21 The structure of the H_2CO molecule

[13] Apart from the point symmetry elements mentioned, the inversion center, horizontal mirror planes and improper axes are possible point symmetry elements.

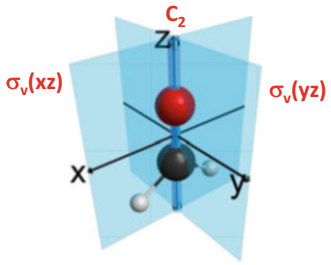

Fig. 10.22 Point symmetry properties of the H_2CO molecule

Table 10.6 Character table of the point group C_{2v}

C_{2v}	$\hat{E}$	$\hat{C}_2$	$\hat{\sigma}_v(xz)$	$\hat{\sigma}_v'(yz)$		
A_1	1	1	1	1	z	x^2,y^2,z^2
A_2	1	1	−1	−1	R_z	xy
B_1	1	−1	1	−1	x, R_y	xz
B_2	1	−1	−1	1	y, R_x	yz

formaldehyde possesses three rotational degrees of freedom. Therefore, the number of vibrational degrees of freedom is $3N - 6 = 6$.

In **subproblem (c)**, we determine the various **symmetry types** of these normal modes. Why symmetry types? Scientists have realized that certain molecular quantities behave differently under application of the molecule's point symmetry operations. The electronic density and the molecular Hamiltonian of H_2CO, for example, are invariant under all four symmetry operations that we have identified. However, quantities such as molecular orbitals may change their sign under rotation or mirror operations. In the point group C_{2v}, there are four different ways for a physical quantity to transform under the possible point symmetry operations. They can thus be classified according to the four symmetry types A_1, A_2, B_1, and B_2. In terms of group theory the latter are the *irreducible representations* of the point group.

The **character table** of the point group breaks down the different transformation behavior of the various symmetry types. It is shown in Table 10.6. Without a detailed harmonic analysis, for example, based on a quantum chemical method, it is possible to evaluate the symmetry types of the six vibrational degrees of freedom. Therefore, we seek the *reducible representation* Γ_{red} of the nuclei's movement and we must decompose it into irreducible representations Γ_i according to:

$$\Gamma_{\text{red}} = \sum_{i=1}^{4} a_i \Gamma_i \tag{10.126}$$

The coefficients a_i are obtained from the reduction formula

$$a_i = \frac{1}{h} \sum \chi_{\text{red}}(\hat{R}) \chi_i(\hat{R}) \tag{10.127}$$

Here, $\chi_i(\hat{R})$ is the character of one of the symmetry operations $\hat{R}$ taken from the character table and χ_{red} is the respective character of the reducible representation for this symmetry operation, and h is the order of the group, which is 4 in this case.

For each symmetry operation $\hat{R}$, we consider the transformation

$$\mathbf{T}(\hat{R})\mathbf{X} = \mathbf{X}' \tag{10.128}$$

where $\mathbf{T}$ is the transformation matrix of the symmetry operation acting on the "vector" $\mathbf{X}$ containing the positions of all nuclei. The character of the symmetry operation sought is simply the trace[14] $\text{Tr}(\mathbf{T}(\hat{R}))$.

The identity operation is represented by a (12×12) unit matrix:

$$\begin{pmatrix}
1&0&0&0&0&0&0&0&0&0&0&0\\
0&1&0&0&0&0&0&0&0&0&0&0\\
0&0&1&0&0&0&0&0&0&0&0&0\\
0&0&0&1&0&0&0&0&0&0&0&0\\
0&0&0&0&1&0&0&0&0&0&0&0\\
0&0&0&0&0&1&0&0&0&0&0&0\\
0&0&0&0&0&0&1&0&0&0&0&0\\
0&0&0&0&0&0&0&1&0&0&0&0\\
0&0&0&0&0&0&0&0&1&0&0&0\\
0&0&0&0&0&0&0&0&0&1&0&0\\
0&0&0&0&0&0&0&0&0&0&1&0\\
0&0&0&0&0&0&0&0&0&0&0&1
\end{pmatrix}
\begin{pmatrix}
x_{\text{O}}\\ y_{\text{O}}\\ z_{\text{O}}\\ x_{\text{C}}\\ y_{\text{C}}\\ z_{\text{C}}\\ x_{\text{H1}}\\ y_{\text{H1}}\\ z_{\text{H1}}\\ x_{\text{H2}}\\ y_{\text{H2}}\\ z_{\text{H3}}
\end{pmatrix}
=
\begin{pmatrix}
x_{\text{O}}\\ y_{\text{O}}\\ z_{\text{O}}\\ x_{\text{C}}\\ y_{\text{C}}\\ z_{\text{C}}\\ x_{\text{H1}}\\ y_{\text{H1}}\\ z_{\text{H1}}\\ x_{\text{H2}}\\ y_{\text{H2}}\\ z_{\text{H3}}
\end{pmatrix} \tag{10.129}$$

and it is immediately obvious that the trace is $\text{Tr}\left(\mathbf{T}(\hat{E})\right) = 12$ and thus $\chi_{\text{red}}(\hat{E}) = 12$. For the other symmetry operations, considerable simplifications are possible. The trace of the transformation matrix is only determined by its diagonal elements, whereas the off-diagonal elements are not important. Only those nuclei that are not displaced during the symmetry operation thus contribute to the trace and we can confine the analysis to these nuclei. For example, a rotation by 180° displaces the hydrogens H1 and H2, whereas the oxygen and carbon are not displaced. The x and y coordinates of the latter change their sign. The effective transformation is thus:

$$\begin{pmatrix}
-1&0&0&0&0&0\\
0&-1&0&0&0&0\\
0&0&1&0&0&0\\
0&0&0&-1&0&0\\
0&0&0&0&-1&0\\
0&0&0&0&0&1
\end{pmatrix}
\begin{pmatrix}
x_{\text{O}}\\ y_{\text{O}}\\ z_{\text{O}}\\ x_{\text{C}}\\ y_{\text{C}}\\ z_{\text{C}}
\end{pmatrix}
=
\begin{pmatrix}
-x_{\text{O}}\\ -y_{\text{O}}\\ z_{\text{O}}\\ -x_{\text{C}}\\ -y_{\text{C}}\\ z_{\text{C}}
\end{pmatrix} \tag{10.130}$$

[14] See Sect.A.3.16 in the Appendix.

and the trace of the transformation matrix is -2. Thus, $\chi_{\text{red}}(\hat{C}_2) = -2$. The two vertical mirror planes are similarly evaluated. For $\hat{\sigma}_v(xz)$ the sign of the y-coordinate changes (see Fig. 10.22) for carbon and oxygen, and the hydrogens.

$$\begin{pmatrix} 1 & 0 & 0\,0 & 0 & 0\,0 & 0 & 0\,0 & 0 & 0 \\ 0 & -1 & 0\,0 & 0 & 0\,0 & 0 & 0\,0 & 0 & 0 \\ 0 & 0 & 1\,0 & 0 & 0\,0 & 0 & 0\,0 & 0 & 0 \\ 0 & 0 & 0\,1 & 0 & 0\,0 & 0 & 0\,0 & 0 & 0 \\ 0 & 0 & 0\,0 & -1 & 0\,0 & 0 & 0\,0 & 0 & 0 \\ 0 & 0 & 0\,0 & 0 & 1\,0 & 0 & 0\,0 & 0 & 0 \\ 0 & 0 & 0\,0 & 0 & 0\,1 & 0 & 0\,0 & 0 & 0 \\ 0 & 0 & 0\,0 & 0 & 0\,0 & -1 & 0\,0 & 0 & 0 \\ 0 & 0 & 0\,0 & 0 & 0\,0 & 0 & 1\,0 & 0 & 0 \\ 0 & 0 & 0\,0 & 0 & 0\,0 & 0 & 0\,1 & 0 & 0 \\ 0 & 0 & 0\,0 & 0 & 0\,0 & 0 & 0\,0 & -1 & 0 \\ 0 & 0 & 0\,0 & 0 & 0\,0 & 0 & 0\,0 & 0 & 1 \end{pmatrix} \begin{pmatrix} x_{\text{O}} \\ y_{\text{O}} \\ z_{\text{O}} \\ x_{\text{C}} \\ y_{\text{C}} \\ z_{\text{C}} \\ x_{\text{H1}} \\ y_{\text{H1}} \\ z_{\text{H1}} \\ x_{\text{H2}} \\ y_{\text{H2}} \\ z_{\text{H3}} \end{pmatrix} = \begin{pmatrix} x_{\text{O}} \\ -y_{\text{O}} \\ z_{\text{O}} \\ x_{\text{C}} \\ -y_{\text{C}} \\ z_{\text{C}} \\ x_{\text{H1}} \\ -y_{\text{H1}} \\ z_{\text{H1}} \\ x_{\text{H2}} \\ -y_{\text{H2}} \\ z_{\text{H3}} \end{pmatrix} \tag{10.131}$$

The trace of the transformation matrix is 4, and thus $\chi_{\text{red}}(\hat{\sigma}_v(xz)) = 4$. The second vertical mirror plane again displaces the hydrogens, we can leave them aside. The transformation changes the sign of the x-coordinates of carbon and oxygen:

$$\begin{pmatrix} -1 & 0\,0 & 0 & 0\,0 \\ 0 & 1\,0 & 0 & 0\,0 \\ 0 & 0\,1 & 0 & 0\,0 \\ 0 & 0\,0 & -1 & 0\,0 \\ 0 & 0\,0 & 0 & 1\,0 \\ 0 & 0\,0 & 0 & 0\,1 \end{pmatrix} \begin{pmatrix} x_{\text{O}} \\ y_{\text{O}} \\ z_{\text{O}} \\ x_{\text{C}} \\ y_{\text{C}} \\ z_{\text{C}} \end{pmatrix} = \begin{pmatrix} -x_{\text{O}} \\ y_{\text{O}} \\ z_{\text{O}} \\ -x_{\text{C}} \\ y_{\text{C}} \\ z_{\text{C}} \end{pmatrix} \tag{10.132}$$

We therefore obtain $\chi_{\text{red}}(\hat{\sigma}'_v(yz)) = 2$. It is useful to summarize these results in an additional line in the character table, as shown in Table 10.7. With the help of Eq. (10.127), we can determine the coefficients a_i

$$a_{A_1} = \frac{1}{4}\left[12 \cdot 1 + (-2) \cdot 1 + 4 \cdot 1 + 2 \cdot 1\right] = 4 \tag{10.133}$$

Table 10.7 Character table of the point group C_{2v}

C_{2v}	$\hat{E}$	$\hat{C}_2$	$\hat{\sigma}_v(xz)$	$\hat{\sigma}'_v(yz)$		
A_1	1	1	1	1	z	x^2,y^2,z^2
A_2	1	1	-1	-1	R_z	xy
B_1	1	-1	1	-1	x, R_y	xz
B_2	1	-1	-1	1	y, R_x	yz
Γ_{red}	12	-2	4	2		

$$a_{A_2} = \frac{1}{4}\left[12 \cdot 1 + (-2) \cdot 1 + 4 \cdot (-1) + 2 \cdot (-1)\right] = 1 \tag{10.134}$$

$$a_{B_1} = \frac{1}{4}\left[12 \cdot 1 + (-2) \cdot (-1) + 4 \cdot 1 + 2 \cdot (-1)\right] = 4 \tag{10.135}$$

$$a_{B_2} = \frac{1}{4}\left[12 \cdot 1 + (-2) \cdot (-1) + 4 \cdot (-1) + 2 \cdot 1\right] = 3 \tag{10.136}$$

As a consequence, the reducible representation is reduced into irreducible representations according to:

$$\Gamma_{\text{red}} = 4A_1 + A_2 + 4B_1 + 3B_2. \tag{10.137}$$

However, the movements we have analyzed also contain translations and rotations of the molecule as a whole. The character table reveals the symmetry types of the translations x, y, z, in addition to rotations R_x, R_y, R_z in the last column. The representation of the translations and rotations are

$$\Gamma_{\text{trans}} = A_1 + B_1 + B_2 \tag{10.138}$$

$$\Gamma_{\text{rot}} = A_2 + B_1 + B_2 \tag{10.139}$$

By subtraction of the latter we obtain the result for the vibrations:

$$\Gamma_{\text{vib}} = \Gamma_{\text{red}} - \Gamma_{\text{trans}} - \Gamma_{\text{rot}} = 3A_1 + 2B_1 + B_2. \tag{10.140}$$

We come to the conclusion that three normal modes have the symmetry type A_1, two modes are of type B_1, and one mode has symmetry type B_2. In fact, an elaborate harmonic analysis of the molecule based on quantum chemical methods would confirm this result. Why might this information be useful? Just one application of this result is the prediction of infrared activity in **subproblem (d)**. Infrared active modes and the translations x, y, and z share the same symmetry type. The information is found in the character tables. All six of the normal modes are infrared active. Moreover, a vibrational mode is Raman active if its symmetry type corresponds to one of the products x^2, y^2, z^2, xy,xz, or yz. The latter information can also be taken from the character table. We conclude that all modes of formaldehyde are also Raman active.

The six normal modes of H_2CO, as they are obtained from a quantum chemical vibrational analysis, are shown in Fig. 10.23. The modes are ordered according to increasing vibrational frequencies. The mode with the lowest frequency ν_1 is a bending mode of symmetry type B_2. The two B_1 modes are a rocking mode ν_2 and the mode ν_6 at highest frequency, which is a asymmetric C-H stretch mode. The three modes of symmetry type A_1 are C-O stretch movements combined with in-phase and out-of-phase scissoring motion of the C-H bonds (ν_3 and ν_4), and the symmetric C-H stretch mode ν_5.

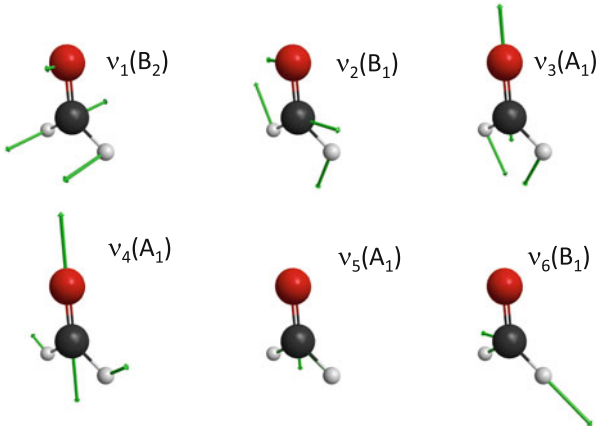

Fig. 10.23 The six normal modes of the H_2CO molecule

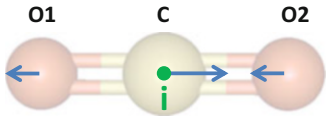

Fig. 10.24 The CO_2 molecule and its asymmetric stretch mode ν_3. If the oxygens O1 and O2 belong to the same isotopic species, then additional selection rules from nuclear spin statistics take effect. One point symmetry element of the molecule is its inversion center *i*. *Arrows* indicate schematically the motion of the ν_3 vibrational mode

Problem 10.9 (Influence of Nuclear Spin Statistics)
The IR absorption of the linear molecule $^{12}C^{16}O_2$ is investigated in the region of the asymmetric stretch mode ν_3 (Fig. 10.24). Near the band center, the first observable rovibrational transition of the P branch is found at 2,347.576 cm^{-1}. The first observable transition of the R branch is found at 2,349.918 cm^{-1}. ^{16}O has zero nuclear spin. The linear molecule with inversion center belongs to the point group $D_{\infty h}$. A character table is given in Table 10.8. The symmetry type of the asymmetric stretch mode is Σ_u^+.

a. Which subsets of rovibrational transitions are forbidden because of nuclear spin statistics?
b. Determine the C-O bond length in CO_2 in its vibrational ground state. Ignore the centrifugal distortion.

Solution 10.9 In this exercise, our attention is drawn to nuclear spin statistics and its influence on the spectra of molecules with symmetric structure. The prominent

Table 10.8 Character table of the point group $D_{\infty h}$, according to [3]

$D_{\infty h}$	$\hat{E}$	$2\hat{C}(\phi)$	$\hat{\sigma}_v$	$\hat{i}$	$2\hat{S}(\phi)$	$\hat{C}_2$		
Σ_g^+	1	1	1	1	1	1		$x^2 + y^2, z^2$
Σ_g^-	1	1	−1	1	1	−1	R_z	
Π_g	2	$2\cos\phi$	0	2	$-2\cos\phi$	0	(R_x, R_y)	(xz, yz)
Δ_g	2	$2\cos 2\phi$	0	2	$2\cos 2\phi$	0		$(x^2 - y^2, xy)$
Σ_u^+	1	1	1	−1	−1	−1	z	
Σ_u^-	1	1	−1	−1	−1	1		
Π_u	2	$2\cos\phi$	0	−2	$2\cos\phi$	0	(x, y)	
Δ_u	2	$2\cos 2\phi$	0	−2	$-2\cos 2\phi$	0		

example is $^{12}C^{16}O_2$ where, as it turns out, every second rovibrational transition is forbidden in the region of the asymmetric stretch band $\nu_3 = 0 \rightarrow 1$.

In **subproblem (a)**, we identify the subset of transitions that are forbidden owing to nuclear spin statistics. For this, we need to bring together the given facts and consider the consequences for the symmetry of the molecule's wave function. Nuclei of the same isotopic species are indistinguishable quantum mechanical objects. In $^{12}C^{16}O_2$, we have a two-particle system of ^{16}O nuclei, which we could label 1 and 2. Now, consider an exchange operator $\hat{T}$ acting on the nuclei's wave function with the result that the particles are exchanged:

$$\hat{T}\psi(1,2) = \tau\psi(2,1); \qquad \tau \in \mathbb{C} \tag{10.141}$$

If the operator acts twice, then the original situation is re-established. This requires a condition for the eigenvalue τ:

$$\hat{T}\hat{T}\psi(1,2) = \hat{T}\tau\psi(2,1) = \tau^2\psi(1,2) = \psi(1,2) \tag{10.142}$$

$$\tau = \begin{cases} +1; \text{ Bosons} \\ -1; \text{ Fermions} \end{cases} \tag{10.143}$$

According to the *spin-statistics theorem*, the case $\tau = +1$ applies to particles with integer spin, whereas the asymmetric case, in which the sign of the wave function changes, applies to particles with half-integral spin. As ^{16}O nuclei have zero nuclear spin and are thus bosons; the sign of their total wave function does not change upon exchange of the particles. For spin 0 particles the nuclear spin wave function is symmetrical. Moreover, the electronic part of the molecule's wave function in the electronic ground state is symmetrical. However, the rotational and the vibrational parts require attention. The rotational wave functions of a linear molecule are the spherical harmonics $Y_{JM}(\theta, \phi)$ with the property of alternating

parity[15] with the rotational quantum number J:

$$\hat{P}Y_{JM}(\theta,\phi) = (-1)^J Y_{JM}(\pi-\theta,\phi+\pi) \tag{10.144}$$

This can easily be checked for low-order spherical harmonics listed in the appendix (Sect. A.3.14). Thus, for even $J = 0, 2, 4, \ldots$, the sign of the rotational part of the total wave function does not change upon inversion, whereas for odd values ($J = 1, 3, \ldots$) it does. The behavior of the vibrational part of the wave function depends on the symmetry of the normal mode and the number of quanta by which it is excited. If we inspect the behavior of the asymmetric stretch mode ν_3 under inversion (see Fig. 10.24) we see that the movement of the nuclei is just reversed under the inversion operation. The latter is a point symmetry element of the molecule. The point group of the molecule is $D_{\infty h}$. In terms of group theory, the symmetry type of the asymmetric stretch mode is Σ_u^+ and the character for the inversion operation is -1, as can be seen from the character table of this point group, Table 10.8. If the number of quanta in this mode is odd ($n = 1, 3, 5, \ldots$), then the symmetry type of the vibrational wave function corresponds to the symmetry type of the normal mode. If, however, the number of quanta in the mode is even—the ground state $n = 0$ included—then the wave function is totally symmetrical and its sign does not change under the inversion operation.[16] Now, we combine this information and consider the relevant parts of the total wave function as a product of vibrational and rotational parts:

$$\hat{P}\psi_{nJ} = \hat{P}\psi_{\mathrm{vib},n}\psi_{\mathrm{rot},J} \stackrel{!}{=} +1\psi_{\mathrm{vib},n}\psi_{\mathrm{rot},J} \tag{10.145}$$

This condition is satisfied if even values of J are combined with even values of n, and, moreover, if odd values of J are combined with odd values of n.

Thus, to answer the question of subproblem (a), nuclear spin statistics forbids rotational states with an odd quantum number J in the vibrational ground state $n_3 = 0$. In the singly excited state $n_3 = 1$, rotational states with even J are forbidden. A term scheme with the first allowed and the forbidden rovibrational transitions of the $^{12}C^{16}O_2$ molecule is shown in Fig. 10.25. Apparently, every second transition is forbidden in the P- and in the R-branches.

With this information we can solve **subproblem (b)**, in which we determine the bond lengths of the two C-O bonds in the vibrational ground state. It turns out that we can fall back on many of the formulas we have used in Problem 10.7. But first we have to consider the differences in the term scheme between diatomics such as CO and linear polyatomic molecules such as CO_2. Clearly, a molecule with more than

[15] The parity operation $\hat{P}$ is an inversion with the result $(x, y, z) \rightarrow (-x, -y, -z)$ or $(r, \theta, \phi) \rightarrow (r, \pi - \theta, \phi + \pi)$.

[16] This follows from the fact that harmonic oscillator wave functions (Eq. (A.76), see also Fig. 9.1), have even parity for even quantum numbers $n = 0, 2, 4, \ldots$, and odd parity for odd quantum numbers $n = 1, 3, 5, \ldots$.

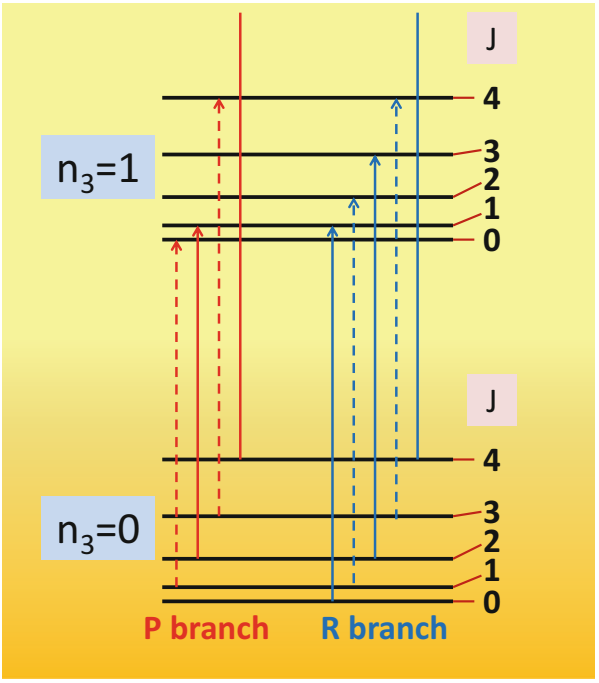

Fig. 10.25 Term scheme (schematic) of the first allowed (*solid lines*) and forbidden rovibrational transitions (*dashed lines*) of the asymmetric stretch vibration for the $^{12}C^{16}O_2$ molecule

two nuclei has more than one single vibrational degrees of freedom. The triatomic carbon dioxide ($N = 3$) has $3N - 5 = 4$ vibrational degrees of freedom. Two of them, the bending modes ν_{2a} and ν_{2b}, are twofold degenerate. The mode ν_1 is the symmetrical stretch mode. In the adaption of Eq. (10.93) to the triatomic case, variable degeneracies d_i of different vibrational modes should thus be considered. Anharmonicity not only implies overtones, but also combinations and their mutual interaction. There are anharmonicity constants x_{ij} for each pair of normal modes. In addition, for each of the normal modes there is a rotation-vibration coupling constant $\alpha_{e,i}$. The adapted expression for the energy levels of the triatomic is thus:

$$\begin{aligned} E_{n_1 n_2 n_3 J} = V(R_e) &+ \sum_{i=1}^{3} h\nu_{e,i}\left(n_i + \frac{d_i}{2}\right) + hB_e J(J+1) \\ &- \frac{1}{2}\sum_{i=1}^{3}\sum_{j=1}^{3} hx_{i,j}\left(n_i + \frac{d_i}{2}\right)\left(n_j + \frac{d_j}{2}\right) - \sum_{i=1}^{3} h\alpha_{e,i}\left(n_i + \frac{d_i}{2}\right) J(J+1) \\ &- h\bar{D}_e J^2 (J+1)^2 . \end{aligned} \tag{10.146}$$

Note the factor $\frac{1}{2}$ in front of the double sum preventing double counting. It is common practice to introduce a rotational constant

$$B_{n_1 n_2 n_3} = B_e - \sum_{i=1}^{3} \alpha_{e,i} \left(n_i + \frac{d_i}{2} \right) \tag{10.147}$$

for the vibrational state, which is the generalization of the constants B_i ($i = 0, 1, 2$) we have used in the diatomic case in Problem 10.7. It is clear that with the sparse information given in this problem, we are not able to determine the equilibrium rotational constant B_e and thus the equilibrium C-O bond distance. This would require determination of the rotation vibration constants $\alpha_{e,i}$ for *all* normal modes. Here we concentrate on the determination of B_{000}, the ground state rotational constant from which the bond length in the ground state can be determined. We must figure out how this is possible with the information of only two line positions in the P- and the R-branches of the transition[17] $000 \rightarrow 001$. At first, the notion is important that for the calculation of a transition frequency between the ground state and the singly excited asymmetric stretch mode many of the terms are unchanged in these two states and thus cancel each other out. With $d_1 = d_3 = 1$ and $d_2 = 2$, we obtain for the P-branch ($J' = J + 1 \rightarrow J$, see the introduction of the number J' in Problem 10.7)

$$\begin{aligned} \Delta\nu &= \frac{E_{001,J} - E_{000,J+1}}{h} \\ &= \nu_{e,3} - 2x_{33} - \frac{1}{2}x_{13} - x_{23} - (B_{001} + B_{000})\, J' + (B_{001} - B_{000})\, J'^2 \end{aligned} \tag{10.148}$$

and for the R-branch ($J \rightarrow J' = J + 1$)

$$\begin{aligned} \Delta\nu &= \frac{E_{001,J+1} - E_{000,J}}{h} \\ &= \nu_{e,3} - 2x_{33} - \frac{1}{2}x_{13} - x_{23} + (B_{001} + B_{000})\, J' + (B_{001} - B_{000})\, J'^2. \end{aligned} \tag{10.149}$$

In the problem text, the wave numbers of the first observable transitions of these branches are given. According to Fig. 10.25 the first observable transition for the P-branch has $J' = 2$, whereas the R-branch starts with $J' = 1$. We therefore obtain two equations

$$\Delta\nu_P = \nu_{e,3} - 2x_{33} - \frac{1}{2}x_{13} - x_{23} + 2B_{001} - 6B_{000} \tag{10.150}$$

[17] Note that there are at least three different methods for the notation of vibrational states of the CO_2 molecule in use in textbooks and in the scientific literature. The notation used in this problem is sufficient here, but it is not the most general one.

and

$$\Delta\nu_R = \nu_{e,3} - 2x_{33} - \frac{1}{2}x_{13} - x_{23} + 2B_{001} \tag{10.151}$$

for the frequencies of these two transitions. By taking the difference between these frequencies and multiplying with the speed of light, we arrive at:

$$c\,(\Delta\tilde{\nu}_R - \Delta\tilde{\nu}_P) = 6B_{000}. \tag{10.152}$$

With $\Delta\tilde{\nu}_R = 2349.918\,\mathrm{cm}^{-1}$ and $\Delta\tilde{\nu}_P = 2347.576\,\mathrm{cm}^{-1}$, the ground state rotational constant is:

$$B_{000} = \frac{1}{6}\times 2.99792458\times 10^{-10}\,\mathrm{cm\,s}^{-1}\times 2.342\,\mathrm{cm}^{-1} = 11701.9\,\mathrm{MHz}. \tag{10.153}$$

It is related via Eq. (10.12) to the moment of inertia of the molecule,

$$I = m_{^{16}\mathrm{O}}\,(-r_{\mathrm{CO}})^2 + m_{^{16}\mathrm{O}}\,(+r_{\mathrm{CO}})^2 = 2m_{^{16}\mathrm{O}}r_{\mathrm{CO}}^2, \tag{10.154}$$

and thus to the ground state bond length sought r_{CO}:

$$r_{\mathrm{CO}} = \sqrt{\frac{h}{8\pi^2 2m_{^{16}\mathrm{O}}B_{000}}} = 1.162\times 10^{-10}\,\mathrm{m} \tag{10.155}$$

Our result for the C-O bond lengths within the CO_2 molecule in its vibrational ground state is thus 1.162 Å.

Problem 10.10 (LASER-I)
Consider an optical resonator containing an active material represented by a four-level system, as shown in Fig. 10.26. The laser transition is between the states $|2\rangle$ and $|1\rangle$. Population inversion between these two states is achieved by pumping from the ground level $|0\rangle$ into the state $|3\rangle$ with a pump rate of R_{03}, followed by relaxation into the state $|2\rangle$ within the decay time T_{32}. The transition $|2\rangle \rightarrow |1\rangle$ is possible either by spontaneous emission (decay time T_{21}) or by stimulated emission with a cross section σ.

a. For efficient laser operation, is it better to choose a system with T_{10} much shorter than T_{21}, or a system with $T_{10} > T_{21}$?
b. An ideal four-level laser can be described by the following rate equations for the population N_2 of the upper state $|2\rangle$ and the photon density Φ:

(continued)

Problem 10.10 (continued)

$$\frac{dN_2}{dt} = -\frac{N_2}{\tau} - \sigma c N_2 \Phi + R \tag{10.156}$$

$$\frac{d\Phi}{dt} = -\frac{\Phi}{\tau_r} + \sigma c N_2 \Phi \tag{10.157}$$

R is the pump rate, i.e., the number of particles per volume and time being excited into the upper level, τ is the lifetime of $|2\rangle$ in the zero field including nonradiative relaxation. The relaxation time τ_r of the photon density accounts for radiative losses in the cavity, including transmission through one of the mirrors where the laser radiation is emitted, and c is the speed of light. Determine the steady-state population of the upper level $|2\rangle$ in addition to the minimum pump rate R_{crit} necessary for operation with a He-Ne laser ($\tau = 1 \times 10^{-8}$ s, $\tau_r = 3 \times 10^{-8}$ s, $\sigma = 3 \times 10^{-13}$ cm^2) and for a Nd:YAG laser ($\tau = 2.5 \times 10^{-4}$ s, $\tau_r = 7 \times 10^{-10}$ s, $\sigma = 8 \times 10^{-19}$ cm^2)

c. Consider small distortions from the steady-state values N_{2s} and Φ_s, $N_2(t) = N_{2s} + n$, and $\Phi(t) = \Phi_s + \phi$. Show that the population distortions can be described by a damped oscillator

$$\frac{d^2 n}{dt^2} + 2\delta \frac{dn}{dt} + \omega^2 n = 0 \tag{10.158}$$

where δ is a damping parameter and ω is the angular frequency of the relaxation oscillations. Compare the relaxation behavior of the He-Ne laser and the Nd:YAG laser using the parameters given above and a pumping rate of $R = 2R_{\text{crit}}$. Which laser shows relaxation oscillations?

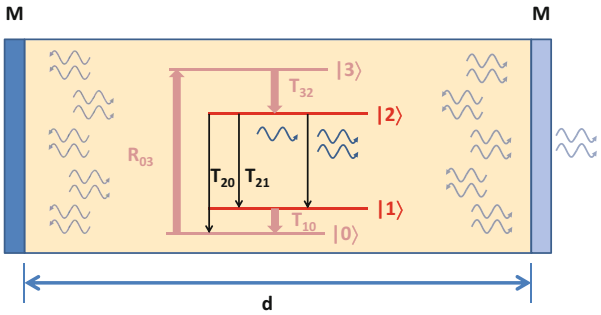

Fig. 10.26 Principle of laser operation (schematic). The active medium is represented by a four-level quantum system within a resonator of d in length. The laser transition is between levels $|2\rangle$ and $|1\rangle$. At least one of the mirrors (M) has nonzero transmission

Solution 10.10 Lasers[18] are an indispensable tool of spectroscopy, as they provide monochromatic coherent light of high intensity. Here, we deal with the principles of laser operation using the model sketched in Fig. 10.26. Within an optical resonator, there is an active medium that is represented by a four-level quantum system. Under operating conditions, the level $|2\rangle$ has a higher population than the lower level $|1\rangle$. This inversion is crucial, as it allows stimulated emission of quanta with the energy $h\nu = E_2 - E_1$ and thus a build-up of radiation within the resonator of this frequency. In the zero field the population inversion would decay owing to spontaneous emission (decay time T_{21}) or because of other nonradiative processes, and reach the population given by the Boltzmann distribution at a certain temperature. An effective mechanism of inversion is achieved by a suitable pump mechanism involving the transition from the ground state $|0\rangle$ to a higher state $|3\rangle$ with the rate R_{03}. Owing to rapid relaxation, the upper laser level $|2\rangle$ is then substantially populated. In **subproblem (a)**, we assess the efficiency of an active medium regarding the decay time of the lower laser level $|1\rangle$. If N_1 and N_2 are the densities of the lower and the upper levels respectively, the degree of inversion is simply the difference $N_2 - N_1$. Now, if the decay time T_{10} were long compared with T_{21}, the lower level $|1\rangle$ would already be populated because of spontaneous emission processes. Thus, the inversion would decrease owing to a flooding of the lower level $|1\rangle$. Therefore, for good laser operation, we need the opposite situation, i.e., a very short lifetime of the level $|1\rangle$, so that ideally, $N_1 = 0$ holds. The answer is thus that $T_{10} \ll T_{21}$ is needed for laser operation. Moreover, simple models like ours assume that the pumping mechanism yields a constant rate by which the upper level $|2\rangle$ is populated. This requires a constant population of the ground state, N_0. Under these conditions, the four-level laser system can be described by the two rate equations Eqs. (10.156) and (10.157). The equation for the time-dependent population density of the upper laser level $|2\rangle$, $N_2(t)$ can be motivated primarily by the rate equations for induced and spontaneous emission (Eqs. (10.8) and (10.9)). The photon density Φ can be related to the spectral energy density $u(\nu)$ introduced in Sect. 10.1.1 via $u(\nu) = h\nu\Phi$. One relevant parameter is the lifetime τ of the level $|2\rangle$, which includes spontaneous decay in addition to nonradiative processes that depopulate this level. Moreover, the time τ_r describes the decay of the photon density caused by imperfect reflectivity of the mirrors, dissipation, and, of course, losses due to coupling out of the radiation because of transmission through at least one of the mirrors. The first terms on the right-hand side of Eqs. (10.156) and (10.157) describe these loss mechanisms of N_2 and Φ respectively. However, the photon density is fed by means of stimulated emission with the cross section σ, represented by the second term in Eq. (10.157). This gain is proportional to N_2, which in turn decreases by the same amount (second term in Eq. (10.156)). The constant pumping rate R increases N_2 (third term in Eq. (10.156)). Apparently, we do not account for details such as an index of refraction that is different from unity. We assume that electromagnetic waves propagate through the resonator at the vacuum speed of light c. Here, it

[18]The word *laser* is the abbreviation for light amplification by stimulated emission of radiation.

is worth mentioning that these laser equations are similar to those describing the Lotka-Volterra kinetic model of oscillating chemical reactions that we have dealt with in Problems 6.6 and 6.7. Hence, in the following, we benefit from what we have worked out in chemical kinetics. It is not easy to solve these coupled equations without numerical methods.

The first point we examine in **subproblem (b)** are the stationary solutions. These are characterized by a constant population N_{2s} of the upper laser level, and a constant photon density Φ_s. The first derivatives of these quantities are thus zero. Taking Eq. (10.157), we obtain:

$$0 = -\frac{\Phi_s}{\tau_r} + \sigma c N_{2s} \Phi_s \tag{10.159}$$

which yields the stationary state population

$$N_{2s} = \frac{1}{\sigma c \tau_r}. \tag{10.160}$$

Interestingly, within this simple model N_{2s} does not depend on the pump rate R; it depends only on the cross section for stimulated emission and the decay time of Φ. For a He-Ne gas laser with $\tau_r = 3 \times 10^{-8}$ s and $\sigma = 3 \times 10^{-13}$ cm^2 we obtain:

$$N_{2s}^{\text{He–Ne}} = 4 \times 10^9 \,\text{cm}^{-3}. \tag{10.161}$$

For a Nd:YAG solid-state laser the steady-state density is:

$$N_{2s}^{\text{Nd:YAG}} = \frac{1}{8 \times 10^{-19}\,\text{cm}^2 \times 3 \times 10^{10}\,\text{cm}\,\text{s}^{-1} \times 7 \times 10^{-10}\,\text{s}} = 6 \times 10^{16}\,\text{cm}^{-3}. \tag{10.162}$$

Note that τ_r does not depend on the active material, but on the quality of the resonator. Next, we determine the critical pump rate above which laser operation is observed. The latter requires $\Phi_s > 0$. Insertion of Eq. (10.160) in Eq. (10.156) yields an expression for the photon density as a function of the pump rate:

$$\Phi_s = \tau_r R - \frac{1}{\sigma c \tau} \tag{10.163}$$

From the condition $\Phi_s \stackrel{!}{=} 0$, we obtain the critical pump rate

$$R_{\text{crit}} = \frac{1}{\sigma c \tau \tau_r} = \frac{N_{2s}}{\tau} \tag{10.164}$$

For the He-Ne gas laser, we obtain:

$$R_{\text{crit}}^{\text{He–Ne}} = 4 \times 10^{17}\,\text{cm}^{-3}\,\text{s}^{-1}. \tag{10.165}$$

For the Nd:YAG laser, the critical pump rate is orders of magnitude higher:

$$R_{\text{crit}}^{\text{Nd:YAG}} = 2 \times 10^{20}\,\text{cm}^{-3}\,\text{s}^{-1}. \tag{10.166}$$

On the one hand, the Nd:YAG laser has a much longer lifetime of the upper laser level, which reduces R_{crit}, but this is overcompensated for by the much smaller cross section for stimulated emission. Different types of lasers may also differ in their dynamic behavior, which we investigate in **subproblem (c)**. We examine how the system behaves if the steady-state values of N_2 and Φ_s are distorted by small deviations n and ϕ respectively. We show that the systems behave like a damped oscillator. If we insert $N_2(t) = N_{2s} + n(t)$ in Eq. (10.156) we obtain

$$\frac{dN_2(t)}{dt} = \frac{dn(t)}{dt} = -\frac{N_{2s}}{\tau} - \frac{n(t)}{\tau} - \sigma c\,(N_{2s} + n(t))\,(\Phi_s + \phi(t)) + R \tag{10.167}$$

and thus

$$\begin{aligned}\frac{dn(t)}{dt} &= \underbrace{-\frac{N_{2s}}{\tau} - \sigma c N_{2s}\Phi_s + R}_{=0} - \frac{n(t)}{\tau} - \sigma c\Phi_s n(t) - \sigma c N_{2s}\phi(t) - \underbrace{\sigma c n(t)\phi(t)}_{\text{neglected}} \\ &= -\frac{n(t)}{\tau} - \sigma c\Phi_s n(t) - \sigma c N_{2s}\phi(t).\end{aligned} \tag{10.168}$$

The nonlinear term containing the product $n(t)\phi(t)$ is ignored, as n and ϕ are considered to be small distortions. In the same way, we treat Eq. (10.157) and obtain

$$\begin{aligned}\frac{d\phi(t)}{dt} &= -\frac{\Phi_s}{\tau_r} - \frac{\phi(t)}{\tau_r} + \sigma c\,(N_{2s} + n(t))\,(\Phi_s + \phi(t)) \\ &= \underbrace{-\frac{\Phi_s}{\tau_r} + \sigma c N_{2s}\Phi_s}_{=0} - \frac{\phi(t)}{\tau_r} + \sigma c\Phi_s n(t) + \sigma c N_{2s}\phi(t) + \underbrace{\sigma c n(t)\phi(t)}_{\text{neglected}} \\ &= -\frac{\phi(t)}{\tau_r} + \sigma c \underbrace{N_{2s}}_{=\frac{1}{\sigma c \tau_r}}\phi(t) + \sigma c\Phi_s n(t) \\ &= \sigma c\Phi_s n(t)\end{aligned} \tag{10.169}$$

Now, by taking the derivative of Eq. (10.168), we obtain

$$\frac{d^2 n(t)}{dt^2} = -\left(\frac{1}{\tau} + \sigma c\Phi_s\right)\frac{dn(t)}{dt} - \sigma c\frac{1}{\sigma c\tau_r}\frac{d\phi(t)}{dt} \tag{10.170}$$

and by substitution of the derivative of $\phi(t)$ using Eq. (10.169), we arrive at

$$\frac{d^2 n(t)}{dt^2} + \left(\frac{1}{\tau} + \sigma c \Phi_s\right) \frac{d n(t)}{dt} + \frac{\sigma c}{\tau_r} \Phi_s n(t) = 0 \tag{10.171}$$

This differential equation has the form Eq. (10.158). It describes damped oscillations with angular frequency

$$\omega = \sqrt{\frac{\sigma c}{\tau_r} \Phi_s} \tag{10.172}$$

and damping parameter

$$\delta = \frac{1}{2}\left(\frac{1}{\tau} + \sigma c \Phi_s\right) \tag{10.173}$$

For the analysis of the dynamic behavior we assume a pump rate that is twice the critical pump rate for laser operation. With $R = 2R_{\text{crit}}$ the angular relaxation, frequency is

$$\omega = \sqrt{\frac{1}{\tau \tau_r}} \tag{10.174}$$

and the damping parameter is

$$\delta = \frac{1}{\tau} \tag{10.175}$$

Now we solve Eq. (10.158), which is a homogeneous differential equation with constant coefficients. The general solution is:

$$n(t) = c_1 \mathrm{e}^{\lambda_1 t} + c_2 \mathrm{e}^{\lambda_2 t} \tag{10.176}$$

where the constants c_1 and c_2 follow from the initial conditions. The parameters λ_1 and λ_2 are the roots of the characteristic polynomial

$$\lambda^2 + 2\delta\lambda + \omega^2 = 0 \tag{10.177}$$

which we obtain using Eq. (A.4):

$$\lambda_{1,2} = -\delta \pm \sqrt{\delta^2 - \omega^2} \tag{10.178}$$

Now we need to consider two cases regarding the sign of the discriminant $\delta^2 - \omega^2$. If it is positive then λ_1 and λ_2 are real and the solution for the initial condition

$n(t=0)=n_0$ is[19]

$$n(t)=n_0\mathrm{e}^{-\delta t}\cosh\left(\sqrt{\delta^2-\omega^2}t\right). \tag{10.179}$$

If, however, $\delta^2-\omega^2$ is negative, then λ_1 and λ_2 are complex conjugate numbers, $\lambda_1=-\delta+i\sqrt{\omega^2-\delta^2}$ and $\lambda_2=-\delta-i\sqrt{\omega^2-\delta^2}$. Insertion in Eq. (10.176) reveals the damped oscillatory behavior of $n(t)$ in this case[20]:

$$n(t)=n_0\mathrm{e}^{-\delta t}\cos\left(\sqrt{\omega^2-\delta^2}t\right) \tag{10.180}$$

With the parameters τ and τ_r given for the He-Ne laser and the Nd:YAG laser we can calculate ω and δ according to Eqs. (10.174) and (10.175). The results are given in Table 10.9. For the Nd:YAG laser ω largely exceeds the damping parameter δ for the assumed pump rate. This laser type thus exhibits relaxation oscillations, as shown in Fig. 10.27. The oscillations have a frequency of:

$$\frac{1}{2\pi}\sqrt{\omega^2-\delta^2}\approx 380\,\mathrm{kHz} \tag{10.181}$$

Table 10.9 Parameters influencing the dynamic behavior of lasers concerning small deviations from the stationary state

Laser type	τ (s)	τ_r (s)	ω (rad s^{-1})	δ (s^{-1})	Relaxation oscillations
He-Ne	1×10^{-8}	3×10^{-8}	5.7×10^{7}	10^{8}	No
Nd:YAG	2.5×10^{-4}	7×10^{-10}	2.4×10^{6}	4×10^{3}	Yes

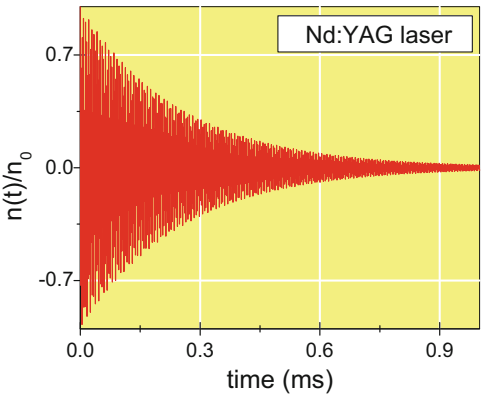

Fig. 10.27 Relaxation dynamics for the Nd:YAG laser, calculated with Eq. (10.180) and the parameters given in the text. Small distortions decay in a damped oscillation within the time scale of 1 ms

[19]Note that the hyperbolic cosine function is defined $\cosh x=\frac{1}{2}\left(\mathrm{e}^{x}+\mathrm{e}^{-x}\right)$.

[20]Note that $\cos x=\frac{1}{2}\left(\mathrm{e}^{ix}+\mathrm{e}^{-ix}\right)$ (see Eq. (A.11) in the appendix).

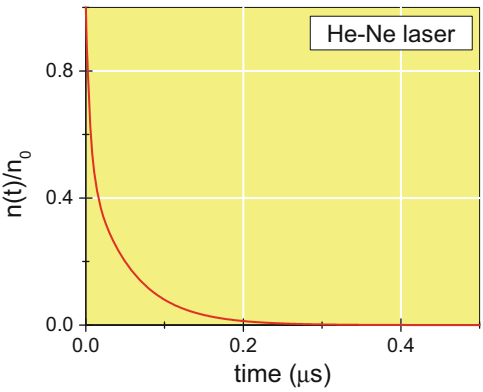

Fig. 10.28 Relaxation dynamics for the He-Ne laser, calculated using Eq. (10.179) and the parameters given in the text. Small distortions $n(t)$ are damped out within the time range of 1 μs

and decay within 1 ms. In contrast, in the case of the He-Ne laser, small distortions from the stationary state are damped out within 1 μs without oscillating behavior, as illustrated in Fig. 10.28.

In the next problem, a numerical solution of the laser equations is examined that confirm the oscillatory behavior around the stationary state seen in the case of the Nd:YAG laser.

Problem 10.11 (LASER-II)
This problems assumes that you have dealt with Problem 10.10. Consider the four-level laser model introduced in Problem 10.10 (Fig. 10.26). Solve the laser equations

$$\frac{dN_2}{dt} = -\frac{N_2}{\tau} - \sigma c N_2 \Phi + R \tag{10.182}$$

$$\frac{d\Phi}{dt} = -\frac{\Phi}{\tau_r} + \sigma c N_2 \Phi \tag{10.183}$$

for the population of the upper laser level N_2 and the photon density in the oscillator Φ numerically either by using mathematical software or by writing a computer code based, for example, on the Runge-Kutta scheme of integration (see appendix Sect. A.3.18). Examine the switch-on behavior of the Nd:YAG laser by selecting the initial conditions $N_2 = 0$ and $\Phi(t = 0) = \epsilon$ where ϵ is a small positive number. Use parameters given in Problem 10.10, simulate on a time scale that covers a few milliseconds, and assume a pump rate $R = 5R_{\text{crit}}$. Why do you need $\epsilon > 0$? Can you explain the complex switch-on behavior?

Solution 10.11 This exercise assumes that you have already dealt with Problem 10.10, where the principle of laser light sources was investigated and a stationary solution for the rate equations Eqs. (10.182) and (10.183) was determined. In addition, small deviations from the stationary state values N_{2s} and Φ_s could be treated by neglecting the nonlinearity in these equations. A full solution of these equations requires, however, numerical methods. As for the Lotka-Volterra model for oscillating chemical reactions in Problem 6.7 we can use the Runge-Kutta method (Sect. A.3.18) to integrate Eqs. (10.182) and (10.183) into a discrete grid with a time step interval $h = t_{n+1} - t_n$ ($n = 1, 2, \ldots$). Starting from the initial values $N_2(0) = 0$ and $\Phi(0) = 0$, we investigate the switch-on behavior of the Nd:YAG laser. In Problem 10.10 we have seen that this type of laser shows the tendency toward relaxation oscillations. If the pumping is switched on at $t = 0$, the laser is far from its stationary state and it is interesting to examine how the stationary state is established. There is a hint given that we assume a small initial value of the photon density $\Phi(0) = \epsilon$. The reason becomes clear if we inspect Eq. (10.183): the gain of the photon density described by the second term is proportional to Φ. Hence, if $\Phi = 0$ then the photon density stays exactly zero for $t > 0$. We have thus to start from a small photon density ϵ, say $\Phi(0) = 0.1$, resulting, for example, from noise in the resonator. An analogous problem does not occur for N_2 because the gain term of N_2 is the constant pump rate R. For the simulation, we assume a pump rate of $R = 5R_{\text{crit}}$. Let us calculate the expected stationary state values N_{2s} and Φ_s. The stationary population density N_{2s} is independent of R and takes the value $5.96 \times 10^{16}\,\text{cm}^{-3}$ (see Eq. (10.162)). By means of Eq. (10.163) we obtain:

$$\Phi_s = \tau_r R - \frac{1}{\sigma c \tau} = \tau_r 5R_{\text{crit}} - \frac{1}{\sigma c \tau} \overset{\text{Eq. (10.164)}}{=} \frac{4}{\sigma c \tau} = 6.7 \times 10^{11}\,\text{cm}^{-3}, \qquad (10.184)$$

where we have used the parameters $\sigma = 8 \times 10^{-19}\,\text{cm}^2$ and $\tau = 2.5 \times 10^{-4}\,\text{s}^{-1}$. For the simulation, it is crucial that the integration of Eqs. (10.182) and (10.183) is performed on a fine grid, e.g., $h = 10^{-11}$ s. Results of the simulation are shown in Figs. 10.29 and 10.30. N_2 starts from zero and continuously grows to reach a value of $1.2 \times 10^{17}\,\text{cm}^{-3}$. During this time period, the photon density in the resonator is

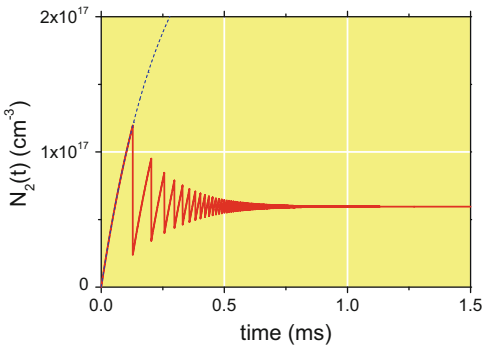

Fig. 10.29 Switch-on behavior of an Nd:YAG laser obtained from a numerical simulation based on Eqs. (10.182) and (10.183). The population of the upper laser level as a function of time is shown. The *dashed line* is the behavior according to Eq. (10.186)

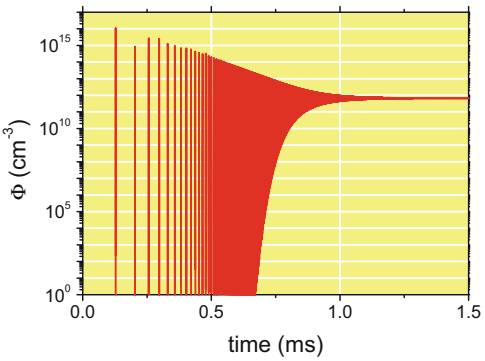

Fig. 10.30 Switch-on behavior of an Nd:YAG laser obtained from a numerical simulation based on Eqs. (10.182) and (10.183). The photon density within the resonator is shown to be a function of time. Note the logarithmic scale for Φ

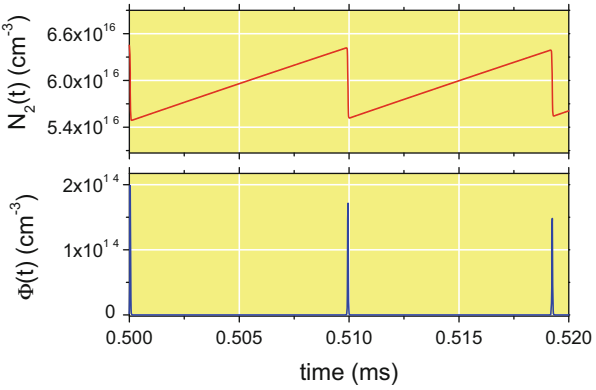

Fig. 10.31 Population of the upper laser level N_2 and photon density Φ as a function of time. Snapshot of the simulation between 0.5 and 0.52 ms.

close to zero. At $t \approx 0.13$ ms, however, Φ exhibits a sharp *spike* and N_2 is suddenly reduced to about $2.5 \times 10^{16}\,\mathrm{cm}^{-3}$, increases again until at 0.21 ms, the population of the upper laser level is again suddenly reduced, accompanied by another spike in the photon density. This pattern is repeated in the following, with the tendency that the time between consecutive spikes of Φ and setbacks of N_2 respectively, becomes shorter and shorter. In Fig. 10.31, a snapshot of the simulation between 0.50 and 0.52 ms is shown where the sawtooth-like variation of N_2 and the spikes of the photon density are seen in more detail.

Next, we examine the dynamic behavior in detail. The appearance of spikes is related to the coupling between the population density N_2 and the photon density Φ, which is initially negligibly small for a long period. During this period the coupling term in Eq. (10.182) can be omitted:

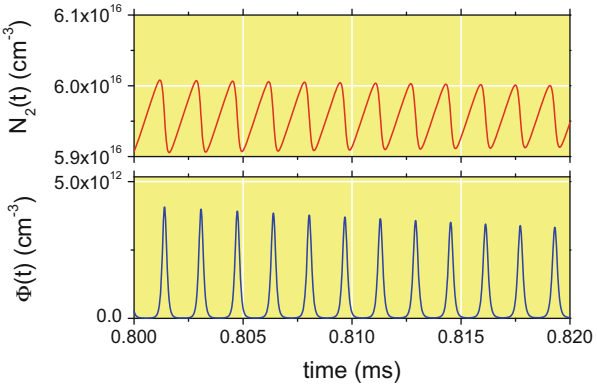

Fig. 10.32 Population of the upper laser level N_2 and photon density Φ as a function of time. Snapshot of the simulation between 0.8 and 0.82 ms

$$\frac{d\,N_2}{dt} + \frac{N_2}{\tau} \approx R \tag{10.185}$$

The solution of this inhomogeneous differential equation is given by (see also appendix Sect. A.3.18)

$$N_2(t) \approx R\tau \left(1 - \mathrm{e}^{-\frac{t}{\tau}}\right) = 5N_{2s} \left(1 - \mathrm{e}^{-\frac{t}{\tau}}\right) \tag{10.186}$$

where we have made use of Eq. (10.164). The limiting behavior according to Eq. (10.186) is also shown in Fig. 10.29 as a dashed line. It is in line with the simulation result, until after about 0.13 ms, the coupling with the photon density comes into effect and causes the immediate depopulation of the upper level and a momentary increase in Φ. Then, however, the photon density decays rapidly with a time constant of $\tau_r = 7 \times 10^{-10}$ s, and Φ reaches a value of nearly zero within this time scale. As the upper laser level was not completely depopulated, the recovery of N_2 starts from a higher value until the next spike appears.

Figure 10.32 shows the behavior between 0.80 and 0.82 ms. The repetition rate of spikes has become higher, and they are wider. In Fig. 10.33, where a snapshot of the simulation between 1.20 and 1.22 ms is shown, N_2 and Φ exhibit a nearly harmonic oscillatory behavior around the stationary state values calculated above.

Looking back on our results we were able to numerically solve the laser equations and to simulate the switch-on behavior of the Nd:YAG laser including the appearance of spikes and the relaxation from a highly nonlinear behavior into the stationary state. Oscillations around the stationary state treated in Problem 10.11 are confirmed by the simulation.

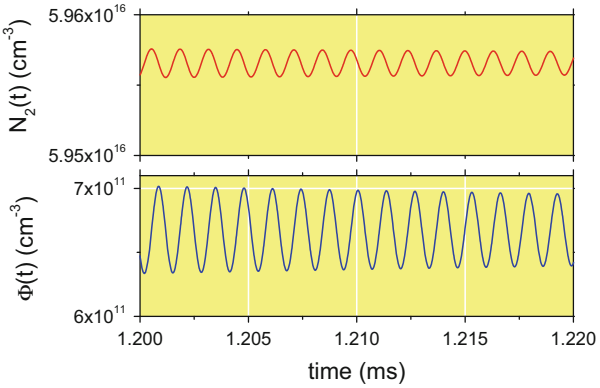

Fig. 10.33 Population of the upper laser level N_2 and photon density Φ as a function of time. Snapshot of the simulation between 1.2 and 1.22 ms

References

1. Louisell WH (1973) Quantum statistical properties of radiation. Wiley, New York
2. Edmonds AR (1957) Angular momentum in quantum mechanics. Princeton University Press, Princeton
3. McHale JL (1999) Molecular spectroscopy. Prentice Hall, Upper Saddle River